This article has been accepted for publication in a future issue of this journal, but has not been fully edited. Content may change prior to final publication.
Citation information: DOI: 10.1109/TCYB.2025.3626066, IEEE Transactions on Cybernetics

Zonotopic Set-Membership Fusion Estimation for Complex Networks: A Buffer-Aided Strategy

Zhongyi Zhao, Zidong Wang, Jinling Liang, and Wenying Xu

***Abstract*—This paper is concerned with the zonotopic set-membership fusion estimation (SMFE) problem for a class of complex networks (CNs). The measurements of the CNs are transmitted to a remote fusion center through a shared communication network. Due to the limited network bandwidth, the transmissions of the measurement information occur intermittently, and the nodes' transmission intervals may exceed their sampling periods. To enhance the utilization of the measurement information, each node of the CN is equipped with a buffer for real-time data storage, so that the fusion center can utilize more measurement information at time instants when the node's transmission interval is larger than its sampling period. The aim of this paper is to design SMFE algorithms based on both the parallel fusion scheme and the data compression fusion scheme, respectively, using the data received at the fusion center. Firstly, by iterating the state equation of the CN, a batch processing method is proposed to process the input data of the fusion center concurrently. Subsequently, by employing the zonotopic set-membership estimation technique, the desired SMFE algorithms are designed. Moreover, sufficient criteria are established to ensure that the sizes of the output zonotopes of the SMFE algorithms remain uniformly bounded. Finally, two numerical examples are presented to illustrate the effectiveness of the proposed algorithms.**

***Index Terms*—Zonotopic set-membership estimation, fusion estimation, complex networks, buffer-aided strategy.**

I. INTRODUCTION

Complex networks (CNs) are regarded as systems composed of nodes through which information is exchanged with neighboring nodes according to certain topologies. It is widely acknowledged that CNs can model a broad range of practical systems, such as power grids [31], social networks [44], and artificial neural networks [50]. Consequently, considerable research attention has been directed towards CNs, resulting in a wealth of significant findings, see, e.g., [4], [10], [19], [21], [25], [37], [38]. Among these research areas, state estimation has attracted particular interest, owing primarily to the importance of CNs' state information in various practical applications, such as estimator-based control and fault detection [13], [14], [32], [39]. Up to now, numerous research results concerning the state estimation of CNs have been reported in the literature, see [38] for locally minimized variance estimation, [34] for H_∞ estimation, and [42] for set-membership estimation (SME).

In recent years, the SME of CNs has attracted increasing research interest because the SME technique requires only the bounds of noises rather than their precise statistical characteristics. Consequently, numerous related results have been reported in the literature, see [8], [17], [18], [43], [53] and the references therein. For instance, in [8], the dynamic event-triggered fault estimation issue was studied for a class of nonlinear time-varying CNs by employing the ellipsoidal SME technique. Through the recursive solution of linear matrix inequalities, ellipsoidal sets restraining faults were obtained. Unlike ellipsoids, which are often not closed under the Minkowski sum and linear mapping operations (two essential set operations in SME), zonotopes possess this closure property [9], [36], [49]. Motivated by this advantage, the zonotopic SME for CNs was investigated in [43], [53].

From the perspective of multi-sensor fusion, a CN can be viewed as a multi-sensor system, where each node of the CN has a measurement output corresponding to a sensor node. To date, most of the existing results concerning the state estimation of CNs have been obtained using the parallel fusion scheme. Estimators designed under the parallel fusion scheme are often straightforward to implement and possess optimality in certain senses [1], [2], [29], [45], [47]. Nevertheless, the adoption of the parallel fusion scheme in estimator design may result in a heavy computational burden, particularly for large-scale systems such as CNs. To address this issue, the sequential fusion scheme was employed in [52] to design an SME algorithm for CNs subject to uniform quantization. In addition to the sequential fusion scheme, the data compression fusion scheme has been demonstrated as another fusion approach capable of effectively reducing computational burden [15], [33]. Furthermore, such a scheme can achieve the same estimation accuracy as that of the parallel fusion scheme through appropriate design [28]. In light of these observations, it is a natural idea to investigate the set-membership fusion estimation (SMFE) problem of CNs under the data compression fusion scheme.

For decades, with the rapid development of network technologies, numerous state estimation algorithms have been designed based on the measurements received from commu-

This work was supported in part by the National Natural Science Foundation of China under Grants 62373103, 62403130, and 62573121; in part by the Jiangsu Provincial Scientific Research Center of Applied Mathematics of China under Grant BK20233002; in part by the Natural Science Foundation of Jiangsu Province of China under Grant BK20241286; in part by the Jiangsu Funding Program for Excellent Postdoctoral Talent of China under Grant 2024ZB601; in part by the China Postdoctoral Science Foundation-CCTEG Joint Support Program under Grant 2025T055ZGMK; in part by the Royal Society of the UK; and in part by the Alexander von Humboldt Foundation of Germany. (*Corresponding author: Jinling Liang*)

Zhongyi Zhao, Jinling Liang and Wenying Xu are with the School of Mathematics, Southeast University, Nanjing 210096, China. (Emails: zhongyizhao@seu.edu.cn, jinlliang@seu.edu.cn, wyxu@seu.edu.cn)

Zidong Wang is with the Department of Computer Science, Brunel University London, Uxbridge, Middlesex, UB8 3PH, U.K. (Email: Zidong.Wang@brunel.ac.uk)

nication networks, see, e.g., [3], [7], [11], [20], [22], [26]. In network-based estimation, the limited bandwidth often results in transmission intervals of the measurement signals that exceed the sampling periods, thereby causing a degradation in estimation performance [30], [54]. To mitigate this issue, the buffer-aided strategy has been demonstrated as an effective approach [35], [40], [48]. In this strategy, the measurement outputs of a sensor are stored in a buffer in real time, and all the accumulated data are transmitted to the estimator simultaneously when transmission is permitted. In this manner, a greater amount of measurement information can be utilized in the design of the estimator, thus allowing the estimation performance to be enhanced through proper design, and this motivates the application of the buffer-aided strategy to the zonotopic SMFE.

Based on the above discussions, the buffer-aided zonotopic SMFE for CNs is investigated in this paper. Two fundamental challenges are identified as follows:

1) How to design zonotopic SMFE algorithms for CNs equipped with buffers under the parallel and data compression fusion schemes?
2) How to analyze the steady-state performance of the SMFE algorithms?

Accordingly, the main contributions of this paper are summarized as follows:

1) The zonotopic SMFE problem is addressed, for the first time, for CNs operating under a buffer-aided strategy.
2) A novel batch processing method is developed to handle the measurement data from buffers. In contrast to the re-estimation-based method in [40], the proposed approach allows the simultaneous use of buffered measurements, thereby facilitating the subsequent design of the SMFE algorithms.
3) Two centralized SMFE algorithms are constructed based on the parallel fusion scheme and the data compression scheme, respectively. In contrast to the matrix-inequality-based methods in [35], [48], the proposed algorithms achieve optimality in the sense of minimizing the F-radii of the output zonotopes. Furthermore, the recursive structure of the algorithms makes them suitable for online implementation.
4) Sufficient criteria applicable to unstable CNs are derived to ensure the uniform boundedness of the F-radii of the output zonotopes generated by the proposed SMFE algorithms under both fusion schemes.

The remainder of this paper is organized as follows. Section II presents the CN model, the transmission model under the buffer-aided strategy, and the objectives of the paper. In Section III, a batch processing method is introduced to process the data from the buffers of the considered CN, followed by the design of a parallel SMFE algorithm and a data-compression SMFE algorithm. Subsequently, an analysis is conducted to examine the uniform boundedness of the sizes of the output zonotopes produced by the SMFE algorithms. Section IV provides two numerical examples to verify the effectiveness of the proposed SMFE algorithms. Finally, Section V concludes the paper based on the obtained findings.

Notations: $\mathbb{N}_+$ and $\mathbb{N}$ denote the set of positive integers and the set of natural numbers, respectively. $\mathrm{vec}_\chi\{\Pi^{(\xi)}\} \triangleq \left[(\Pi^{(1)})^T \ (\Pi^{(2)})^T \ \cdots \ (\Pi^{(\chi)})^T\right]^T$ and $\mathrm{diag}_\chi\{\Pi^{(\xi)}\} \triangleq \mathrm{diag}\{\Pi^{(1)}, \Pi^{(2)}, \ldots, \Pi^{(\chi)}\}$ for matrices $\Pi^{(\xi)}$ $(\xi = 1, 2, \ldots, \chi)$ of proper dimensions. For a set $\mathscr{I} \subset \{1, 2, \ldots, \chi\}$ and matrices $\Pi^{(\xi)}$ $(\xi = 1, 2, \ldots, \chi)$, $\mathrm{vec}^\chi_{\xi\in\mathscr{I}}\{\Pi^{(\xi)}\}$ and $\mathrm{diag}^\chi_{\xi\in\mathscr{I}}\{\Pi^{(\xi)}\}$ denote the matrix after removing the row blocks $\Pi^{(\xi)}$ $(\xi \notin \mathscr{I})$ from $\mathrm{vec}_\chi\{\Pi^{(\xi)}\}$ and the matrix after removing the diagonal blocks $\Pi^{(\xi)}$ $(\xi \notin \mathscr{I})$ from $\mathrm{diag}_\chi\{\Pi^{(\xi)}\}$, respectively. For sets $Z_1, Z_2, \ldots, Z_n \subset \mathbb{R}^n$ and a matrix $Y \in \mathbb{R}^{m\times n}$, $Z_1 \oplus Z_2 \triangleq \{z_1 + z_2 : z_1 \in Z_1, z_2 \in Z_2\}$; $Y \odot Z_1 \triangleq \{Yz_1 : z_1 \in Z_1\}$; $\bigoplus_{i\in\{1,2,\ldots,N\}} Z_i \triangleq Z_1 \oplus Z_2 \oplus \cdots \oplus Z_N$. The operation "$\odot$" is granted a higher precedence than "$\oplus$". For a matrix Z with total n rows, $\mathrm{rs}\{Z\} \triangleq \mathrm{diag}_n\{\|Z_\xi\|_\infty\}$ with Z_ξ being the ξ-th row of Z. $\mathbf{1}$ is a column vector composed of ones.

II. PRELIMINARIES AND PROBLEM FORMULATION

A. Preliminaries and System Model

In this paper, zonotopes are employed to bound the external noises and the system states, whose definition is provided as follows.

Definition 1: [24] An m-order zonotope with center $d \in \mathbb{R}^n$ and generator matrix $D \in \mathbb{R}^{n\times m}$, denoted as $\langle d, D\rangle$, is defined as

$$\langle d, D\rangle \triangleq \{d + D\varphi : \varphi \in \mathbb{R}^m, \|\varphi\|_\infty \le 1\}.$$

Consider a class of CNs composed of N nodes, where the dynamics of the i-th node are described as follows:

$$x_i(k+1) = A_i(k)x_i(k) + \sum_{j=1}^{N} \lambda_{ij}(k)\Theta(k)x_j(k) + w_i(k) \tag{1}$$

$$y_i(k) = C_i(k)x_i(k) + v_i(k) \tag{2}$$

$$x_i(0) \in \langle 0, X_i(0)\rangle \tag{3}$$

where $x_i(k) \in \mathbb{R}^n$ and $y_i(k) \in \mathbb{R}^m$ denote the state and the measurement output, respectively; and $w_i(k)$ and $v_i(k)$ denote the external process and measurement noises satisfying

$$w_i(k) \in \langle 0, W_i(k)\rangle \tag{4}$$

$$v_i(k) \in \langle 0, V_i(k)\rangle \tag{5}$$

with $W_i(k)$ and $V_i(k)$ being positive diagonal matrices. $\lambda_{ij}(k)$ describes the coupling strength from node j to node i, which satisfies $\lambda_{ij}(k) > 0$ if the information can be transmitted from node j to node i or otherwise $\lambda_{ij}(k) = 0$. $\Theta(k) \triangleq \mathrm{diag}_n\{\theta_\xi(k)\} \in \mathbb{R}^{n\times n}$ stands for the inner coupling matrix with $\theta_\xi(k) > 0$ for each $\xi \in \{1, 2, \ldots, n\}$; $A_i(k)$ and $C_i(k)$ are known matrices; and $X_i(0)$ is a known positive diagonal matrix.

Remark 1: The parameters $X_i(0)$, $W_i(k)$, and $V_i(k)$ $(i = 1, 2, \ldots, N)$ must be selected sufficiently large to guarantee that (3)–(5) are satisfied. Otherwise, the SME performance cannot be guaranteed. Meanwhile, these parameters should be chosen such that the zonotopes in (3)–(5) remain as tight as possible to improve estimation performance. To this end, they

can be set based on prior knowledge such as physical system constraints or measurement accuracy.

B. Transmissions Under the Buffer-Aided Strategy

For each node of the CN in (1) and (2), the measurement output $y_i(k)$ ($i \in \{1, 2, \ldots, N\}$) is transmitted to the remote fusion center via a shared communication network. Due to the limited bandwidth resources, $y_i(k)$ cannot always be allowed to access the communication network at every time instant k. In other words, for each node of the CN, a transmission interval that is larger than a sampling period may occur, during which the node is unable to transmit its measurement information. To address this issue, a buffer-aided strategy is employed to improve the utilization rate of the measurement information for the CN. Under this strategy, each node of the CN is equipped with a buffer, and the signal transmissions of the i-th node are subject to the following constraints.

1) At time instant k, the measurement signal $y_i(k)$ is stored in a buffer with capacity M_i. If the signals stored in the buffer have reached the capacity M_i, then the oldest data (i.e., $y_i(k - M_i)$) are discarded to make room for storing $y_i(k)$.
2) The signals stored in the buffer are required to wait for permission to access the communication network. Once the buffer is granted access, all signals in the buffer are sent to the fusion center, after which the buffer is emptied..

To model the input of the fusion center, a monotonically increasing sequence $\{\eta_{i,t}\}_{t=1}^{\infty}$ is introduced to represent the transmission time instants when the buffer of the i-th node of the CN is permitted to access the network. The following assumption is made regarding the transmission intervals.

Assumption 1: [51] For the buffer of the i-th node, the following constraint holds:

$$\Delta\eta_{i,t} \triangleq \eta_{i,t} - \eta_{i,t-1} \leq \bar{\eta}_i,\ \forall t \in \mathbb{N}_+$$

where $\eta_{i,0} = 0$ and $\bar{\eta}_i$ is a known positive integer.

Under Assumption 1, at time instant $\eta_{i,t}$, the input of the fusion center received from the buffer corresponding to the i-th node is described by the following set:

$$\mathscr{Y}_i(\eta_{i,t}) \triangleq \{y_i(\eta_{i,t}), \ldots, y_i(\eta_{i,t} - \kappa_{i,t} + 1)\} \tag{6}$$

where $\kappa_{i,t} \triangleq \min\{M_i, \Delta\eta_{i,t}\}$.

Define the set of nodes of the CN whose buffers send data to the fusion center at time instant k as

$$\mathscr{I}(k) \triangleq \{i \in \{1, 2, \ldots, N\} : \exists t \in \mathbb{N}_+,\ \text{s.t. } \eta_{i,t} = k\}.$$

Then, the set of all input signals of the fusion center at time instant k is given by

$$\bar{\mathscr{Y}}(k) \triangleq \bigcup_{i \in \mathscr{I}(k)} \mathscr{Y}_i(k). \tag{7}$$

Remark 2: Obviously, the buffer-aided strategy can effectively improve the utilization of the measurement information. To be more specific, for the i-th node of the CN in (1)–(3), during the time interval from $k = 0$ to $k = \eta_{i,t'}$ ($t' \in \mathbb{N}_+$), the total number of signals received by the fusion center is $\sum_{t=1}^{t'} \kappa_{i,t} + 1$ when using the buffer-aided strategy, compared to $\eta_{i,t'} + 1$ without it.

C. Problem Statement

The objectives of this paper are threefold:

1) To propose a batch processing method for handling the input signals received by the fusion center.
2) To design zonotopic set-membership fusion estimators for the CN in (1) and (2) under the parallel and data compression fusion schemes, respectively, by utilizing the proposed batch processing method.
3) To establish sufficient criteria to ensure the uniform boundedness of the sizes of the output zonotopes generated by the designed estimation algorithms.

III. MAIN RESULTS

A. Batch Processing of Data Received by the Fusion Center

In this subsection, a batch processing method will be proposed to process the signals in the set $\bar{\mathscr{Y}}(k)$ at each time instant k.

Define $\mathbf{x}(k) \triangleq \text{vec}_N\{x_i(k)\}$. Then, based on (1)–(3), the dynamics of the entire CN can be obtained as follows:

$$\mathbf{x}(k+1) = \mathcal{A}(k)\mathbf{x}(k) + \bar{w}(k) \tag{8}$$

$$y_i(k) = \bar{C}_i(k)\mathbf{x}(k) + v_i(k),\ i = 1, 2, \ldots, N \tag{9}$$

$$\mathbf{x}(0) \in \langle 0, \tilde{X}(0)\rangle \tag{10}$$

where

$$\mathcal{A}(k) = \text{diag}_N\{A_i(k)\} + \Lambda(k) \otimes \Theta(k)$$
$$\bar{w}(k) = \text{vec}_N\{w_i(k)\}$$
$$\tilde{X}(0) = \text{diag}_N\{X_i(0)\}$$
$$\bar{C}_i(k) = [\underbrace{0_{m\times n} \ \ldots \ 0_{m\times n}}_{i-1} \ \ C_i(k) \ \ \underbrace{0_{m\times n} \ \ldots \ 0_{m\times n}}_{N-i}]$$
$$\Lambda(k) = \begin{bmatrix} \lambda_{11}(k) & \cdots & \lambda_{1N}(k) \\ \vdots & \ddots & \vdots \\ \lambda_{N1}(k) & \cdots & \lambda_{NN}(k) \end{bmatrix}.$$

Additionally, according to (4), one can easily derive from Definition 1 that the noise term $\bar{w}(k)$ in (8) satisfies

$$\bar{w}(k) \in \langle 0, \bar{W}(k)\rangle \tag{11}$$

where $\bar{W}(k) = \text{diag}_N\{W_i(k)\}$.

Now, let us employ a monotonically increasing sequence $\{\bar{k}_t\}_{t=1}^{\infty}$ to represent the sequence of time instants when $\bar{\mathscr{Y}}(\bar{k}_t) \neq \emptyset$. It follows from (8) that

$$\mathbf{x}(\bar{k}_{t+1}) = \mathscr{A}(\bar{k}_{t+1}, \bar{k}_t)\mathbf{x}(\bar{k}_t) + \mathscr{B}(\bar{k}_{t+1}, \bar{k}_t)\mathbf{w}(\bar{k}_{t+1}, \bar{k}_t) \tag{12}$$

with

$$\mathscr{A}(\bar{k}_{t+1}, \bar{k}_t) = \mathcal{A}(\bar{k}_{t+1} - 1)\mathcal{A}(\bar{k}_{t+1} - 2)\cdots\mathcal{A}(\bar{k}_t)$$
$$\mathscr{B}(\bar{k}_{t+1}, \bar{k}_t) = \begin{bmatrix} \mathscr{A}^T(\bar{k}_{t+1}, \bar{k}_t + 1) \\ \mathscr{A}^T(\bar{k}_{t+1}, \bar{k}_t + 2) \\ \vdots \\ \mathscr{A}^T(\bar{k}_{t+1}, \bar{k}_{t+1} - 1) \\ I \end{bmatrix}^T$$
$$\mathbf{w}(\bar{k}_{t+1}, \bar{k}_t) = \begin{bmatrix} \bar{w}^T(\bar{k}_t) & \cdots & \bar{w}^T(\bar{k}_{t+1} - 1) \end{bmatrix}^T.$$

Furthermore, define $\Delta\bar{k}_t \triangleq \bar{k}_t - \bar{k}_{t-1}$ for $t \in \mathbb{N}_+$ with $\bar{k}_0 \triangleq 0$. For each $i \in \mathscr{I}(\bar{k}_{t+1})$, there exists a $t' \in \mathbb{N}_+$ such that $\eta_{i,t'} = \bar{k}_{t+1}$. Let

$$\mathbf{y}_i(\bar{k}_{t+1}) \triangleq \begin{bmatrix} y_i(\bar{k}_{t+1}) \\ y_i(\bar{k}_{t+1}-1) \\ \vdots \\ y_i(\bar{k}_{t+1}-\iota_{i,t+1}+1) \end{bmatrix}$$

with $\iota_{i,t+1} = \min\{\kappa_{i,t'}, \Delta\bar{k}_{t+1}\}$. The measurement information from the i-th buffer can be expressed as

$$\mathbf{y}_i(\bar{k}_{t+1}) = \mathscr{C}_i(\bar{k}_{t+1})\mathbf{x}(\bar{k}_t) + \mathscr{D}_i(\bar{k}_{t+1})\vec{\mathbf{w}}_i(\bar{k}_{t+1}) + \vec{v}_i(\bar{k}_{t+1}) \tag{13}$$

where

$$\mathscr{C}_i(\bar{k}_{t+1}) = \begin{bmatrix} \bar{C}_i(\bar{k}_{t+1})\mathscr{A}(\bar{k}_{t+1},\bar{k}_t) \\ \bar{C}_i(\bar{k}_{t+1}-1)\mathscr{A}(\bar{k}_{t+1}-1,\bar{k}_t) \\ \vdots \\ \bar{C}_i(\bar{k}_{t+1}-\iota_{i,t+1}+1)\mathscr{A}(\bar{k}_{t+1}-\iota_{i,t+1}+1,\bar{k}_t) \end{bmatrix}$$

$$\begin{aligned}&\mathscr{D}_i(\bar{k}_{t+1}) \\ &= \mathrm{diag}\{\bar{C}_i(\bar{k}_{t+1})\mathscr{B}(\bar{k}_{t+1},\bar{k}_t), \bar{C}_i(\bar{k}_{t+1}-1)\mathscr{B}(\bar{k}_{t+1}-1,\bar{k}_t), \\ &\qquad \ldots, \bar{C}_i(\bar{k}_{t+1}-\iota_{i,t+1}+1)\mathscr{B}(\bar{k}_{t+1}-\iota_{i,t+1}+1,\bar{k}_t)\} \\ &\vec{\mathbf{w}}_i(\bar{k}_{t+1}) = \begin{bmatrix}\mathbf{w}^T(\bar{k}_{t+1},\bar{k}_t) & \cdots & \mathbf{w}^T(\bar{k}_{t+1}-\iota_{i,t+1}+1,\bar{k}_t)\end{bmatrix}^T \\ &\vec{v}_i(\bar{k}_{t+1}) = \begin{bmatrix}v_i^T(\bar{k}_{t+1}) & \cdots & v_i^T(\bar{k}_{t+1}-\iota_{i,t+1}+1)\end{bmatrix}^T.\end{aligned}$$

Remark 3: By iterating the state equation in (8), an equivalent measurement equation of the measurement data received from the i-th buffer is obtained in (13), through which the batch processing of $\mathbf{y}_i(\bar{k}_{t+1})$ can be performed. It should be noted that the established batch processing method is applicable to multi-sensor systems whose buffers may have different transmission time instants, and thus significantly differs from that used for single-sensor systems in [51]. Furthermore, compared with the re-estimation method in [35], [40], [48], which requires re-estimating the system states by using the received signals successively according to their time indices in increasing order, the proposed batch processing method provides greater convenience for the design of the SMFE algorithms.

B. SNE Algorithm Under the Parallel Fusion Scheme

In this subsection, a set-membership estimator is designed for the system in (8)–(9) under the parallel fusion scheme.

Based on (8), (12), and (13), the desired estimator is constructed as follows:

Case 1: For $k \notin \{\bar{k}_t\}_{t=1}^{\infty}$, let

$$\hat{x}(k) = \mathcal{A}(k-1)\hat{x}(k-1) \tag{14}$$

where $\hat{x}(k)$ denotes the estimate of the state $\mathbf{x}(k)$.

Case 2: There exists a nonnegative integer t such that $k = \bar{k}_{t+1}$. Let

$$\begin{aligned}\hat{x}(\bar{k}_{t+1}) = \mathscr{A}(\bar{k}_{t+1},\bar{k}_t)\hat{x}(\bar{k}_t) + \sum_{i\in\mathscr{I}(\bar{k}_{t+1})} K_i(\bar{k}_{t+1}) \\ \times \Big(\mathbf{y}_i(\bar{k}_{t+1}) - \mathscr{C}_i(\bar{k}_{t+1})\hat{x}(\bar{k}_t)\Big)\end{aligned} \tag{15}$$

where $K_i(\bar{k}_{t+1})$ $(i \in \mathscr{I}(\bar{k}_{t+1}))$ are the estimator parameters to be designed.

Define the estimation error as $e(k) \triangleq \mathbf{x}(k) - \hat{x}(k)$. To give the zonotopes enclosing $e(k)$, the following lemma is introduced.

Lemma 1: [23] For zonotopes $\langle d_1, D_1\rangle, \langle d_2, D_2\rangle \subset \mathbb{R}^n$ and matrix $Z \in \mathbb{R}^{m\times n}$, the following properties hold:

$$\begin{aligned}\langle d_1, D_1\rangle \oplus \langle d_2, D_2\rangle &= \langle d_1 + d_2, \begin{bmatrix} D_1 & D_2\end{bmatrix}\rangle \\ Z \odot \langle d_1, D_1\rangle &= \langle Zd_1, ZD_1\rangle.\end{aligned}$$

In the following two theorems, a method will be given to calculate the zonotopes containing $e(k)$ $(k \in \mathbb{N}_+)$.

Theorem 1: For a time instant $k \in \{\bar{k}_t+1, \bar{k}_t+2, \ldots, \bar{k}_{t+1}-1\}$, if

$$e(k-1) \in \langle 0, E(k-1)\rangle \tag{16}$$

then

$$\begin{aligned}e(k) &\in \langle 0, \begin{bmatrix}\mathcal{A}(k-1)E(k-1) & \bar{W}(k-1)\end{bmatrix}\rangle \\ &\triangleq \langle 0, E(k)\rangle.\end{aligned} \tag{17}$$

Proof: It follows from (8) and (14) that, when $k \in \{\bar{k}_t + 1, \bar{k}_t + 2, \ldots, \bar{k}_{t+1} - 1\}$, the estimation error $e(k)$ satisfies

$$e(k) = \mathcal{A}(k-1)e(k-1) + \bar{w}(k-1). \tag{18}$$

Based on (11), (16), and (18), it is obtained from Lemma 1 that

$$e(k) \in \mathcal{A}(k-1) \odot \langle 0, E(k-1)\rangle \oplus \langle 0, \bar{W}(k-1)\rangle = \langle 0, E(k)\rangle$$

which ends the proof. ■

Theorem 2: Let the estimator parameters $K_i(\bar{k}_{t+1})$ $(i \in \mathscr{I}(\bar{k}_{t+1}))$ be given. If

$$e(\bar{k}_t) \in \langle 0, E(\bar{k}_t)\rangle \tag{19}$$

then

$$e(\bar{k}_{t+1}) \in \langle 0, E(\bar{k}_{t+1})\rangle \tag{20}$$

where

$$\begin{aligned}E(\bar{k}_{t+1}) &\triangleq \begin{bmatrix}E^{(1)}(\bar{k}_{t+1}) & \cdots & E^{(4)}(\bar{k}_{t+1})\end{bmatrix} \\ E^{(1)}(\bar{k}_{t+1}) &\triangleq \Big(\mathscr{A}(\bar{k}_{t+1},\bar{k}_t) - \sum_{i\in\mathscr{I}(\bar{k}_{t+1})} K_i(\bar{k}_{t+1})\mathscr{C}_i(\bar{k}_{t+1})\Big) \\ &\qquad \times E(\bar{k}_t) \\ E^{(2)}(\bar{k}_{t+1}) &\triangleq -\Big(\mathrm{vec}^N_{i\in\mathscr{I}(\bar{k}_{t+1})}\{(K_i(\bar{k}_{t+1})\mathscr{D}_i(\bar{k}_{t+1}) \\ &\qquad \times \vec{\mathbf{W}}_i(\bar{k}_{t+1}))^T\}\Big)^T \\ E^{(3)}(\bar{k}_{t+1}) &\triangleq -\Big(\mathrm{vec}^N_{i\in\mathscr{I}(\bar{k}_{t+1})}\{(K_i(\bar{k}_{t+1})\vec{V}_i(\bar{k}_{t+1}))^T\}\Big)^T \\ E^{(4)}(\bar{k}_{t+1}) &\triangleq \mathscr{B}(\bar{k}_{t+1},\bar{k}_t)\mathbf{W}(\bar{k}_{t+1})\end{aligned}$$

with

$$\begin{aligned}\vec{\mathbf{W}}_i(\bar{k}_{t+1}) &\triangleq \mathrm{diag}\{\mathbf{W}(\bar{k}_{t+1}), \ldots, \mathbf{W}(\bar{k}_{t+1}-\iota_{i,t+1}+1)\} \\ \mathbf{W}(\bar{k}_{t+1}) &\triangleq \mathrm{diag}\{\bar{W}(\bar{k}_t), \ldots, \bar{W}(\bar{k}_{t+1}-1)\} \\ \vec{V}_i(\bar{k}_{t+1}) &\triangleq \mathrm{diag}\{V_i(\bar{k}_{t+1}), \ldots, V_i(\bar{k}_{t+1}-\iota_{i,t+1}+1)\}\end{aligned}$$

Proof: According to (12) and (15), it follows that

$$\begin{aligned} e(\bar{k}_{t+1}) &= \Big(\mathscr{A}(\bar{k}_{t+1},\bar{k}_t) - \sum_{i\in\mathscr{I}(\bar{k}_{t+1})} K_i(\bar{k}_{t+1})\mathscr{C}_i(\bar{k}_{t+1})\Big)e(\bar{k}_t) \\ &\quad - \sum_{i\in\mathscr{I}(\bar{k}_{t+1})} K_i(\bar{k}_{t+1})\mathscr{D}_i(\bar{k}_{t+1})\vec{\mathbf{w}}_i(\bar{k}_{t+1}) \\ &\quad - \sum_{i\in\mathscr{I}(\bar{k}_{t+1})} K_i(\bar{k}_{t+1})\vec{v}_i(\bar{k}_{t+1}) \\ &\quad + \mathscr{B}(\bar{k}_{t+1},\bar{k}_t)\mathbf{w}(\bar{k}_{t+1},\bar{k}_t). \end{aligned} \tag{21}$$

With (11) and the definition of $\mathbf{w}(\bar{k}_{t+1},\bar{k}_t)$ (below (12)), one has

$$\mathbf{w}(\bar{k}_{t+1},\bar{k}_t) \in \langle 0, \mathbf{W}(\bar{k}_{t+1})\rangle \tag{22}$$

which, together with the definition of $\vec{\mathbf{w}}_i(\bar{k}_{t+1})$ (below (13)), yields

$$\vec{\mathbf{w}}_i(\bar{k}_{t+1}) \in \langle 0, \vec{\mathbf{W}}_i(\bar{k}_{t+1})\rangle. \tag{23}$$

Similarly, one can obtain from (5) and the definition of $\vec{v}_i(\bar{k}_{t+1})$ (below (13)) that

$$\vec{v}_i(\bar{k}_{t+1}) \in \langle 0, \vec{V}_i(\bar{k}_{t+1})\rangle. \tag{24}$$

In light of (19) and (21)–(24), it can be deduced from Lemma 1 that

$$\begin{aligned} e(\bar{k}_{t+1}) &\in \Big(\mathscr{A}(\bar{k}_{t+1},\bar{k}_t) - \sum_{i\in\mathscr{I}(\bar{k}_{t+1})} K_i(\bar{k}_{t+1})\mathscr{C}_i(\bar{k}_{t+1})\Big) \\ &\quad \odot \langle 0, E(\bar{k}_t)\rangle \\ &\quad \bigoplus_{i\in\mathscr{I}(\bar{k}_{t+1})} (-K_i(\bar{k}_{t+1})\mathscr{D}_i(\bar{k}_{t+1})) \odot \langle 0, \vec{\mathbf{W}}_i(\bar{k}_{t+1})\rangle \\ &\quad \bigoplus_{i\in\mathscr{I}(\bar{k}_{t+1})} (-K_i(\bar{k}_{t+1})) \odot \langle 0, \vec{V}_i(\bar{k}_{t+1})\rangle \\ &\quad \oplus \mathscr{B}(\bar{k}_{t+1},\bar{k}_t) \odot \langle 0, \mathbf{W}(\bar{k}_{t+1})\rangle \\ &= \langle 0, E(\bar{k}_{t+1})\rangle. \end{aligned}$$

The proof is now complete. ∎

In the following theorem, the estimator parameters $K_i(\bar{k}_{t+1})$ $(i \in \mathscr{I}(\bar{k}_{t+1}))$ are designed by minimizing the F-radius of the zonotope in (20) (defined as the Frobenius norm of $E(\bar{k}_{t+1})$ [6]).

Theorem 3: Let

$$\mathcal{K}(\bar{k}_{t+1}) \triangleq \Big(\mathrm{vec}^N_{i\in\mathscr{I}(\bar{k}_{t+1})}\{K_i^T(\bar{k}_{t+1})\}\Big)^T.$$

Let $\mathcal{K}(\bar{k}_{t+1})$ be designed as

$$\mathcal{K}(\bar{k}_{t+1}) = \mathscr{A}(\bar{k}_{t+1},\bar{k}_t)E(\bar{k}_t)E^T(\bar{k}_t)\mathcal{C}^T(\bar{k}_{t+1})\Gamma^{-1}(\bar{k}_{t+1}) \tag{25}$$

where

$$\begin{aligned} \mathcal{C}(\bar{k}_{t+1}) &= \mathrm{vec}^N_{i\in\mathscr{I}(\bar{k}_{t+1})}\{\mathscr{C}_i(\bar{k}_{t+1})\} \\ \Gamma(\bar{k}_{t+1}) &= \mathcal{C}(\bar{k}_{t+1})E(\bar{k}_t)E^T(\bar{k}_t)\mathcal{C}^T(\bar{k}_{t+1}) + \Phi(\bar{k}_{t+1}) \end{aligned}$$

with

$$\Phi(\bar{k}_{t+1}) = \mathrm{diag}^N_{i\in\mathscr{I}(\bar{k}_{t+1})}\{\Phi_i(\bar{k}_{t+1})\}$$

$$\begin{aligned} \Phi_i(\bar{k}_{t+1}) &= \mathscr{D}_i(\bar{k}_{t+1})\vec{\mathbf{W}}_i(\bar{k}_{t+1})\vec{\mathbf{W}}_i^T(\bar{k}_{t+1})\mathscr{D}_i^T(\bar{k}_{t+1}) \\ &\quad + \vec{V}_i(\bar{k}_{t+1})\vec{V}_i^T(\bar{k}_{t+1}). \end{aligned}$$

Then, the F-radius of the zonotope $\langle 0, E(\bar{k}_{t+1})\rangle$ in (20) is minimized.

Proof: According to the expression of $E(\bar{k}_{t+1})$ in (20), the square of the F-radius of the zonotope $\langle 0, E(\bar{k}_{t+1})\rangle$ can be calculated as follows:

$$\begin{aligned} &\mathrm{Tr}\{E(\bar{k}_{t+1})E^T(\bar{k}_{t+1})\} \\ &= \mathrm{Tr}\Big\{\Big(\mathscr{A}(\bar{k}_{t+1},\bar{k}_t) - \sum_{i\in\mathscr{I}(\bar{k}_{t+1})} K_i(\bar{k}_{t+1})\mathscr{C}_i(\bar{k}_{t+1})\Big)E(\bar{k}_t) \\ &\quad \times E^T(\bar{k}_t)\Big(\mathscr{A}(\bar{k}_{t+1},\bar{k}_t) - \sum_{i\in\mathscr{I}(\bar{k}_{t+1})} K_i(\bar{k}_{t+1})\mathscr{C}_i(\bar{k}_{t+1})\Big)^T \\ &\quad + \sum_{i\in\mathscr{I}(\bar{k}_{t+1})} K_i(\bar{k}_{t+1})\mathscr{D}_i(\bar{k}_{t+1})\vec{\mathbf{W}}_i(\bar{k}_{t+1}) \\ &\quad \times \vec{\mathbf{W}}_i^T(\bar{k}_{t+1})\mathscr{D}_i^T(\bar{k}_{t+1})K_i^T(\bar{k}_{t+1}) \\ &\quad + \sum_{i\in\mathscr{I}(\bar{k}_{t+1})} K_i(\bar{k}_{t+1})\vec{V}_i(\bar{k}_{t+1})\vec{V}_i^T(\bar{k}_{t+1})K_i^T(\bar{k}_{t+1}) \\ &\quad + \mathscr{B}(\bar{k}_{t+1},\bar{k}_t)\mathbf{W}(\bar{k}_{t+1})\mathbf{W}^T(\bar{k}_{t+1})\mathscr{B}^T(\bar{k}_{t+1},\bar{k}_t)\Big\}. \end{aligned} \tag{26}$$

With the definition of $\mathcal{K}(\bar{k}_{t+1})$, (26) can be further expressed as

$$\begin{aligned} &\mathrm{Tr}\{E(\bar{k}_{t+1})E^T(\bar{k}_{t+1})\} \\ &= \mathrm{Tr}\Big\{\Big(\mathscr{A}(\bar{k}_{t+1},\bar{k}_t) - \mathcal{K}(\bar{k}_{t+1})\mathcal{C}(\bar{k}_{t+1})\Big)E(\bar{k}_t) \\ &\quad \times E^T(\bar{k}_t)\Big(\mathscr{A}(\bar{k}_{t+1},\bar{k}_t) - \mathcal{K}(\bar{k}_{t+1})\mathcal{C}(\bar{k}_{t+1})\Big)^T \\ &\quad + \mathcal{K}(\bar{k}_{t+1})\Phi(\bar{k}_{t+1})\mathcal{K}^T(\bar{k}_{t+1}) \\ &\quad + \mathscr{B}(\bar{k}_{t+1},\bar{k}_t)\mathbf{W}(\bar{k}_{t+1})\mathbf{W}^T(\bar{k}_{t+1})\mathscr{B}^T(\bar{k}_{t+1},\bar{k}_t)\Big\} \\ &= \mathrm{Tr}\Big\{\Big(\mathcal{K}^T(\bar{k}_{t+1}) - \Gamma^{-1}(\bar{k}_{t+1})\mathcal{C}(\bar{k}_{t+1})E(\bar{k}_t) \\ &\quad \times E^T(\bar{k}_t)\mathscr{A}^T(\bar{k}_{t+1},\bar{k}_t)\Big)^T\Gamma(\bar{k}_{t+1}) \\ &\quad \times \Big(\mathcal{K}^T(\bar{k}_{t+1}) - \Gamma^{-1}(\bar{k}_{t+1})\mathcal{C}(\bar{k}_{t+1})E(\bar{k}_t) \\ &\quad \times E^T(\bar{k}_t)\mathscr{A}^T(\bar{k}_{t+1},\bar{k}_t)\Big) \\ &\quad + \mathscr{A}(\bar{k}_{t+1},\bar{k}_t)E(\bar{k}_t)E^T(\bar{k}_t)\mathscr{A}^T(\bar{k}_{t+1},\bar{k}_t) \\ &\quad - \mathscr{A}(\bar{k}_{t+1},\bar{k}_t)E(\bar{k}_t)E^T(\bar{k}_t)\mathcal{C}^T(\bar{k}_{t+1}) \\ &\quad \times \Gamma^{-1}(\bar{k}_{t+1})\mathcal{C}(\bar{k}_{t+1})E(\bar{k}_t)E^T(\bar{k}_t)\mathscr{A}^T(\bar{k}_{t+1},\bar{k}_t) \\ &\quad + \mathscr{B}(\bar{k}_{t+1},\bar{k}_t)\mathbf{W}(\bar{k}_{t+1})\mathbf{W}^T(\bar{k}_{t+1})\mathscr{B}^T(\bar{k}_{t+1},\bar{k}_t)\Big\}. \end{aligned} \tag{27}$$

From (27), it can be observed that, when $\mathcal{K}(\bar{k}_{t+1})$ is designed according to (25), the F-radius of the zonotope $\langle 0, E(\bar{k}_{t+1})\rangle$ in (20) is minimized, thereby completing the proof. ∎

As a summary of the above results, the following algorithm (Algorithm 1) is provided.

Remark 4: The computational complexity of Algorithm 1 mainly comes from the calculation of $\mathcal{K}(\bar{k}_{t+1})$ in (25). The number of floating-point operations (FLOPs) required for computing $\mathcal{K}(\bar{k}_{t+1})$ is $O(n^2N^2\aleph(\bar{k}_t) + (\sum_{i\in\mathscr{I}(\bar{k}_{t+1})} m\iota_{i,t+1})^3)$. Here, $\aleph(\bar{k}_t)$ denotes the number of columns of $E(\bar{k}_t)$, which

Algorithm 1: SME algorithm under the parallel fusion scheme

Input: Matrix $\tilde{X}(0)$ in (10).
Output: $\hat{x}(k)$, $E(k)$.
Initialization: Give the maximum simulation time $k_{\max}$. Set $k=0$, $\hat{x}(0)=0$, $E(0)=\tilde{X}(0)$.
for $k=1,2,\ldots,k_{\max}$ **do**
  if $\mathscr{I}(k)=\emptyset$ **then**
    Compute $\hat{x}(k)$ by (14);
    Compute $E(k)$ in (17);
  else
    Compute $K_i(k)$ by (25);
    Compute $\hat{x}(k)$ by (15);
    Compute $E(k)$ in (20);

is determined as follows: 1) $\aleph(0)=nN$; and 2) compared with $E(k-1)$, the increment in the number of columns of $E(k)$ is nN when $k\notin\{\bar{k}_t\}_{t=1}^{\infty}$, and $\sum_{i\in\mathscr{I}(\bar{k}_{t+1})}\Delta\bar{k}_{t+1}\iota_{i,t+1}nN+\sum_{i\in\mathscr{I}(\bar{k}_{t+1})}\iota_{i,t+1}m+\Delta\bar{k}_{t+1}nN$ when $k\in\{\bar{k}_t\}_{t=1}^{\infty}$.

C. Estimator Design Under Data Compression Fusion Scheme

In this subsection, an estimator is designed for the CN in (8)–(10) under the data compression fusion scheme. To this end, the method for compressing signals $\mathbf{y}_i(\bar{k}_{t+1})$ ($i\in\mathscr{I}(\bar{k}_{t+1})$) is first provided. Define

$$\vec{\mathbf{y}}(\bar{k}_{t+1})\triangleq\mathrm{vec}^N_{i\in\mathscr{I}(\bar{k}_{t+1})}\{\mathbf{y}_i(\bar{k}_{t+1})\}.$$

According to (13), $\vec{\mathbf{y}}(\bar{k}_{t+1})$ can be expressed as

$$\vec{\mathbf{y}}(\bar{k}_{t+1})=\mathcal{C}(\bar{k}_{t+1})\mathbf{x}(\bar{k}_t)+\mathcal{D}(\bar{k}_{t+1})\overleftarrow{\mathbf{w}}(\bar{k}_{t+1})+\overleftarrow{v}(\bar{k}_{t+1}) \tag{28}$$

where

$$\begin{aligned}\mathcal{D}(\bar{k}_{t+1})&=\mathrm{diag}^N_{i\in\mathscr{I}(\bar{k}_{t+1})}\{\mathscr{D}_i(\bar{k}_{t+1})\}\\ \overleftarrow{\mathbf{w}}(\bar{k}_{t+1})&=\mathrm{vec}^N_{i\in\mathscr{I}(\bar{k}_{t+1})}\{\vec{\mathbf{w}}_i(\bar{k}_{t+1})\}\\ \overleftarrow{v}(\bar{k}_{t+1})&=\mathrm{vec}^N_{i\in\mathscr{I}(\bar{k}_{t+1})}\{\vec{v}_i(\bar{k}_{t+1})\}.\end{aligned}$$

Using the full rank decomposition technique, it follows that

$$\mathcal{C}(\bar{k}_{t+1})=\mathcal{G}(\bar{k}_{t+1})\mathcal{H}(\bar{k}_{t+1}) \tag{29}$$

where $\mathcal{G}(\bar{k}_{t+1})$ is a full-column-rank matrix and $\mathcal{H}(k)$ is a full-row-rank matrix.

On the basis of (28) and (29), the weighted least square (WLS) estimation of $\mathcal{H}(\bar{k}_{t+1})\mathbf{x}(\bar{k}_t)$ can be obtained as follows:

$$\acute{\mathbf{y}}(\bar{k}_{t+1})=\arg\min_{\acute{\mathbf{y}}^*}\|\vec{\mathbf{y}}(\bar{k}_{t+1})-\mathcal{G}(\bar{k}_{t+1})\acute{\mathbf{y}}^*\|^2_{P(\bar{k}_{t+1})}.$$

Here, $\acute{\mathbf{y}}(\bar{k}_{t+1})$ is the desired WLS estimate of $\mathcal{H}(\bar{k}_{t+1})\mathbf{x}(\bar{k}_t)$, and $P(\bar{k}_{t+1})$ is a positive definite matrix to be designed. From [55], $\acute{\mathbf{y}}(\bar{k}_{t+1})$ can be obtained as follows:

$$\begin{aligned}\acute{\mathbf{y}}(\bar{k}_{t+1})=&\left(\mathcal{G}^T(\bar{k}_{t+1})P(\bar{k}_{t+1})\mathcal{G}(\bar{k}_{t+1})\right)^{-1}\\&\times\mathcal{G}^T(\bar{k}_{t+1})P(\bar{k}_{t+1})\vec{\mathbf{y}}(\bar{k}_{t+1}).\end{aligned} \tag{30}$$

Then, by inserting (28) into (30), one derives that

$$\acute{\mathbf{y}}(\bar{k}_{t+1})=\mathcal{H}(\bar{k}_{t+1})\mathbf{x}(\bar{k}_t)+\varepsilon(\bar{k}_{t+1}) \tag{31}$$

where

$$\begin{aligned}\varepsilon(\bar{k}_{t+1})=&\left(\mathcal{G}^T(\bar{k}_{t+1})P(\bar{k}_{t+1})\mathcal{G}(\bar{k}_{t+1})\right)^{-1}\mathcal{G}^T(\bar{k}_{t+1})P(\bar{k}_{t+1})\\&\times(\mathcal{D}(\bar{k}_{t+1})\overleftarrow{\mathbf{w}}(\bar{k}_{t+1})+\overleftarrow{v}(\bar{k}_{t+1})).\end{aligned}$$

In the following proposition, a zonotope enclosing $\varepsilon(\bar{k}_{t+1})$ is derived, and the positive definite matrix $P(\bar{k}_{t+1})$ is designed such that the F-radius of the resulting zonotope is minimized.

Proposition 1: The signal $\varepsilon(\bar{k}_{t+1})$ satisfies

$$\varepsilon(\bar{k}_{t+1})\in\langle 0,\widehat{\varepsilon}(\bar{k}_{t+1})\rangle \tag{32}$$

where

$$\begin{aligned}\widehat{\varepsilon}(\bar{k}_{t+1})=&\left(\mathcal{G}^T(\bar{k}_{t+1})P(\bar{k}_{t+1})\mathcal{G}(\bar{k}_{t+1})\right)^{-1}\mathcal{G}^T(\bar{k}_{t+1})P(\bar{k}_{t+1})\\&\times\left[\mathcal{D}(\bar{k}_{t+1})\overleftarrow{\mathbf{W}}(\bar{k}_{t+1})\quad\overleftarrow{V}(\bar{k}_{t+1})\right]\end{aligned}$$

with $\overleftarrow{\mathbf{W}}(\bar{k}_{t+1})=\mathrm{diag}^N_{i\in\mathscr{I}(\bar{k}_{t+1})}\{\vec{\mathbf{W}}_i(\bar{k}_{t+1})\}$ and $\overleftarrow{V}(\bar{k}_{t+1})=\mathrm{diag}^N_{i\in\mathscr{I}(\bar{k}_{t+1})}\{\vec{V}_i(\bar{k}_{t+1})\}$. Moreover, if the matrix $P(\bar{k}_{t+1})$ is chosen as

$$\begin{aligned}P(\bar{k}_{t+1})=&\Big(\mathcal{D}(\bar{k}_{t+1})\overleftarrow{\mathbf{W}}(\bar{k}_{t+1})\overleftarrow{\mathbf{W}}^T(\bar{k}_{t+1})\mathcal{D}^T(\bar{k}_{t+1})\\&+\overleftarrow{V}(\bar{k}_{t+1})\overleftarrow{V}^T(\bar{k}_{t+1})\Big)^{-1}\end{aligned} \tag{33}$$

then the F-radius of the zonotope in (32) is minimized.

Proof: According to (23), (24), and the definitions of $\overleftarrow{\mathbf{w}}(\bar{k}_{t+1})$ and $\overleftarrow{v}(\bar{k}_{t+1})$, it can be easily deduced from Definition 1 that

$$\begin{aligned}\overleftarrow{\mathbf{w}}(\bar{k}_{t+1})&\in\langle 0,\overleftarrow{\mathbf{W}}(\bar{k}_{t+1})\rangle\\ \overleftarrow{v}(\bar{k}_{t+1})&\in\langle 0,\overleftarrow{V}(\bar{k}_{t+1})\rangle\end{aligned}$$

which further infer

$$\begin{aligned}&\varepsilon(\bar{k}_{t+1})\\&\in\left(\mathcal{G}^T(\bar{k}_{t+1})P(\bar{k}_{t+1})\mathcal{G}(\bar{k}_{t+1})\right)^{-1}\mathcal{G}^T(\bar{k}_{t+1})P(\bar{k}_{t+1})\\&\quad\odot(\mathcal{D}(\bar{k}_{t+1})\odot\langle 0,\overleftarrow{\mathbf{W}}(\bar{k}_{t+1})\rangle\oplus\langle 0,\overleftarrow{V}(\bar{k}_{t+1})\rangle)\\&=\langle 0,\widehat{\varepsilon}(\bar{k}_{t+1})\rangle.\end{aligned}$$

With (32), it is known from the matrix Schwarz inequality (see Lemma 1.1 of [5]) that, when $P(\bar{k}_{t+1})$ is given by (33), the F-radius of the zonotope in (32) is minimized. The proof is now complete. ■

After obtaining the compressed signal $\acute{\mathbf{y}}(\bar{k}_{t+1})$, a set-membership estimator is subsequently designed for the system in (8) and (9) as follows.

Case 1: For $k\notin\{\bar{k}_t\}_{t=1}^{\infty}$, let

$$\check{x}(k)=\mathcal{A}(k-1)\check{x}(k-1) \tag{34}$$

where $\check{x}(k)$ denotes the estimate of state $\mathbf{x}(k)$.

Case 2: There exists a nonnegative integer t such that $k=\bar{k}_{t+1}$. Let

$$\begin{aligned}\check{x}(\bar{k}_{t+1})=&\mathscr{A}(\bar{k}_{t+1},\bar{k}_t)\check{x}(\bar{k}_t)+L(\bar{k}_{t+1})\\&\times\left(\acute{\mathbf{y}}(\bar{k}_{t+1})-\mathcal{H}(\bar{k}_{t+1})\check{x}(\bar{k}_t)\right)\end{aligned} \tag{35}$$

where $L(\bar{k}_{t+1})$ is the estimator parameter to be designed.

Defining the estimation error as $\check{e}(k)\triangleq\mathbf{x}(k)-\check{x}(k)$, it is derived from (8), (12), (31), (34), and (35) that

$$\check{e}(k)=\mathcal{A}(k-1)\check{e}(k-1)+\bar{w}(k-1),\text{for }k\notin\{\bar{k}_t\}_{t=1}^{\infty}$$

$$\check{e}(\bar{k}_{t+1}) = \Big(\mathscr{A}(\bar{k}_{t+1},\bar{k}_t) - L(\bar{k}_{t+1})\mathcal{H}(\bar{k}_{t+1})\Big)\check{e}(\bar{k}_t) - L(\bar{k}_{t+1})\varepsilon(\bar{k}_{t+1}) + \mathscr{B}(\bar{k}_{t+1},\bar{k}_t)\mathbf{w}(\bar{k}_{t+1},\bar{k}_t).$$

Similar to Theorems 1–3, the following results can be obtained for the estimator in (34) and (35).

Theorem 4: For a time instant $k \in \{\bar{k}_t+1, \bar{k}_t+2, \ldots, \bar{k}_{t+1}-1\}$, if $\check{e}(k-1) \in \langle 0, \check{E}(k-1)\rangle$, then

$$\check{e}(k) \in \langle 0, \begin{bmatrix}\mathcal{A}(k-1)\check{E}(k-1) & \bar{W}(k-1)\end{bmatrix}\rangle \triangleq \langle 0, \check{E}(k)\rangle. \tag{36}$$

Theorem 5: Let the estimator parameter $L(\bar{k}_{t+1})$ be given. If $\check{e}(\bar{k}_t) \in \langle 0, \check{E}(\bar{k}_t)\rangle$, then one has

$$\check{e}(\bar{k}_{t+1}) \in \langle 0, \check{E}(\bar{k}_{t+1})\rangle \tag{37}$$

where

$$\begin{aligned}
\check{E}(\bar{k}_{t+1}) &\triangleq \begin{bmatrix}\check{E}^{(1)}(\bar{k}_{t+1}) & \check{E}^{(2)}(\bar{k}_{t+1}) & \check{E}^{(3)}(\bar{k}_{t+1})\end{bmatrix}\\
\check{E}^{(1)}(\bar{k}_{t+1}) &\triangleq \Big(\mathscr{A}(\bar{k}_{t+1},\bar{k}_t) - L(\bar{k}_{t+1})\mathcal{H}(\bar{k}_{t+1})\Big)\check{E}(\bar{k}_t)\\
\check{E}^{(2)}(\bar{k}_{t+1}) &\triangleq -L(\bar{k}_{t+1})\widehat{\varepsilon}(\bar{k}_{t+1})\\
\check{E}^{(3)}(\bar{k}_{t+1}) &\triangleq \mathscr{B}(\bar{k}_{t+1},\bar{k}_t)\mathbf{W}(\bar{k}_{t+1}).
\end{aligned}$$

Moreover, if the estimator parameter $L(\bar{k}_{t+1})$ is designed as

$$L(\bar{k}_{t+1}) = \mathscr{A}(\bar{k}_{t+1},\bar{k}_t)\check{E}(\bar{k}_t)\check{E}^T(\bar{k}_t)\mathcal{H}^T(\bar{k}_{t+1})\check{\Gamma}^{-1}(\bar{k}_{t+1}) \tag{38}$$

with

$$\check{\Gamma}(\bar{k}_{t+1}) = \mathcal{H}(\bar{k}_{t+1})\check{E}(\bar{k}_t)\check{E}^T(\bar{k}_t)\mathcal{H}^T(\bar{k}_{t+1}) + \widehat{\varepsilon}(\bar{k}_{t+1})\widehat{\varepsilon}^T(\bar{k}_{t+1})$$

then the F-radius of the zonotope in (37) is minimized.

Based on the above results, the following algorithm is given.

Algorithm 2: SME algorithm under the data compression fusion scheme

Input: Matrix $\tilde{X}(0)$ in (10).
Output: $\check{x}(k)$, $\check{E}(k)$.
Initialization: Give the maximum simulation time $k_{\max}$. Set $k=0$, $\check{x}(0)=0$, $\check{E}(0)=\tilde{X}(0)$.
for $k = 1, 2, \ldots, k_{\max}$ **do**
  if $\mathscr{I}(k) = \emptyset$ **then**
    Compute $\check{x}(k)$ by (34);
    Compute $\check{E}(k)$ by (36);
  else
    Compute $L(k)$ by (38);
    Compute $P(\bar{k}_{t+1})$ by (33);
    Compute $\acute{\mathbf{y}}(\bar{k}_{t+1})$ by (30);
    Compute $\check{x}(k)$ by (35);
    Compute $\check{E}(k)$ in (37);

Remark 5: The analysis of the computational complexity of Algorithm 2 is similar to that of Algorithm 1. Denote $\wp = \operatorname{rank}(\mathcal{H}(\bar{k}_{t+1}))$. Since the number of FLOPs required for computing $\check{\Gamma}^{-1}(\bar{k}_{t+1})$ in Algorithm 2 is $O(\wp^3)$, which is often lower than that for computing $\Gamma^{-1}(\bar{k}_{t+1})$ in Algorithm 1, therefore, the overall complexity of Algorithm 2 is generally lower. The choice between the SME algorithms under the parallel and the data compression fusion schemes is an important issue in practical applications. Algorithm 2 is preferable when lower computational complexity is desired, whereas Algorithm 1 is more suitable when ease of implementation is the primary consideration and computational cost is not a limiting factor.

D. Uniform Boundedness Analysis

In this subsection, the uniform boundedness of the F-radius of the calculated zonotopes by Algorithms 1–2 is analyzed. To this end, the following assumption is made.

Assumption 2: There exist positive scalars $\underline{\alpha}$, $\bar{\alpha}$, $\underline{\beta}$, $\bar{\beta}$, $\bar{\gamma}$, and $\underline{v}$ such that the following matrix inequalities hold for all $k \in \{0\} \cup \mathbb{N}$:

$$\begin{aligned}
&\underline{\alpha}I < \mathcal{A}(k)\mathcal{A}^T(k) < \bar{\alpha}I\\
&\underline{\beta}I \le \bar{W}(k)\bar{W}^T(k) \le \bar{\beta}I\\
&\bar{C}_i^T(k)\bar{C}_i(k) < \bar{\gamma}I, \quad \forall i \in \{1,2,\ldots,N\}\\
&\vec{V}_i(k)\vec{V}_i^T(k) > \underline{v}I.
\end{aligned}$$

With Assumption 2, Proposition 2 is given and used in the boundedness analysis.

Proposition 2: Under Assumption 2, there exist positive scalars $\underline{a}$, $\bar{a}$, $\underline{b}$, $\bar{b}$, and $\bar{c}$ such that the following matrix inequalities hold for all $t \in \{0\} \cup \mathbb{N}_+$:

$$\begin{aligned}
&\underline{a}I < \mathscr{A}(\bar{k}_{t+1},\bar{k}_t)\mathscr{A}^T(\bar{k}_{t+1},\bar{k}_t) < \bar{a}I\\
&\underline{b}I < \mathscr{B}(\bar{k}_{t+1},\bar{k}_t)\mathbf{W}(\bar{k}_{t+1})\mathbf{W}^T(\bar{k}_{t+1})\mathscr{B}^T(\bar{k}_{t+1},\bar{k}_t) < \bar{b}I\\
&\mathcal{C}^T(\bar{k}_{t+1})\mathcal{C}(\bar{k}_{t+1}) < \bar{c}I.
\end{aligned}$$

Proof: Let $\vec{\eta} \triangleq \max_{i\in\{1,2,\ldots,N\}}\bar{\eta}_i$. Then, it can be obtained that

$$\Delta\bar{k}_t \le \vec{\eta}, \ \forall t \in \mathbb{N}_+. \tag{39}$$

According to (39), the definition of $\mathscr{A}(\bar{k}_{t+1},\bar{k}_t)$, and Assumption 2, one has

$$\begin{aligned}
&\mathscr{A}(\bar{k}_{t+1},\bar{k}_t)\mathscr{A}^T(\bar{k}_{t+1},\bar{k}_t)\\
&= \mathcal{A}(\bar{k}_{t+1}-1)\cdots\mathcal{A}(\bar{k}_t)\mathcal{A}^T(\bar{k}_t)\cdots\mathcal{A}^T(\bar{k}_{t+1}-1)\\
&< \bar{\alpha}^{\Delta\bar{k}_{t+1}}I \le (\max\{1,\bar{\alpha}\})^{\vec{\eta}}I \triangleq \bar{a}I
\end{aligned} \tag{40}$$

and

$$\mathscr{A}(\bar{k}_{t+1},\bar{k}_t)\mathscr{A}^T(\bar{k}_{t+1},\bar{k}_t) > \underline{\alpha}^{\Delta\bar{k}_{t+1}}I \ge (\min\{1,\underline{\alpha}\})^{\vec{\eta}}I \triangleq \underline{a}I. \tag{41}$$

With (40), (41), and the definition of $\mathscr{B}(\bar{k}_{t+1},\bar{k}_t)$, it can be seen that

$$\begin{aligned}
&\mathscr{B}(\bar{k}_{t+1},\bar{k}_t)\mathscr{B}^T(\bar{k}_{t+1},\bar{k}_t)\\
&= \sum_{s=1}^{\Delta\bar{k}_{t+1}-1}\mathscr{A}(\bar{k}_{t+1},\bar{k}_t+s)\mathscr{A}^T(\bar{k}_{t+1},\bar{k}_t+s) + I\\
&= [(\Delta\bar{k}_{t+1}-1)\bar{a}+1]I \le [(\vec{\eta}-1)\bar{a}+1]I
\end{aligned} \tag{42}$$

and

$$\mathscr{B}(\bar{k}_{t+1},\bar{k}_t)\mathscr{B}^T(\bar{k}_{t+1},\bar{k}_t) \ge I. \tag{43}$$

From Assumption 2, one has

$$\underline{\beta}I < \mathbf{W}(\bar{k}_{t+1})\mathbf{W}^T(\bar{k}_{t+1}) < \bar{\beta}I$$

which, together with (42) and (43), gives

$$\begin{aligned}\underline{\beta}I &< \mathscr{B}(\bar{k}_{t+1},\bar{k}_t)\mathbf{W}(\bar{k}_{t+1})\mathbf{W}^T(\bar{k}_{t+1})\mathscr{B}^T(\bar{k}_{t+1},\bar{k}_t)\\ &< \bar{\beta}[(\vec{\eta}-1)\bar{a}+1]I.\end{aligned}$$

Therefore, $\underline{b}$ and $\bar{b}$ can be taken as $\underline{\beta}$ and $\bar{\beta}[(\vec{\eta}-1)\bar{a}+1]$, respectively.

In accordance with the definition of $\mathcal{C}(\bar{k}_{t+1})$, it follows that

$$\begin{aligned}&\mathcal{C}^T(\bar{k}_{t+1})\mathcal{C}(\bar{k}_{t+1})\\ &= \sum_{i\in\mathscr{I}(\bar{k}_{t+1})}\mathscr{C}_i^T(\bar{k}_{t+1})\mathscr{C}_i(\bar{k}_{t+1})\\ &= \sum_{i\in\mathscr{I}(\bar{k}_{t+1})}\sum_{s=1}^{\iota_{i,t+1}}\mathscr{A}^T(\bar{k}_{t+1}+1-s,\bar{k}_t)\bar{C}_i^T(\bar{k}_{t+1}+1-s)\\ &\qquad\times\bar{C}_i(\bar{k}_{t+1}+1-s)\mathscr{A}(\bar{k}_{t+1}+1-s,\bar{k}_t)\\ &< N\bar{a}\bar{\gamma}\iota_{i,t+1}I \le N\bar{a}\bar{\gamma}\vec{\eta}I \triangleq \bar{c}I.\end{aligned}$$

The proof is now complete. ∎

In addition to Proposition 2, the following lemma is also useful in the boundedness analysis.

Lemma 2: [16] For square matrices Υ_1, Υ_3 and matrices Υ_2, Υ_4 of proper dimensions, assume that Υ_1, Υ_3, and $\Upsilon_1+\Upsilon_2\Upsilon_3\Upsilon_4$ are invertible. Then, the following equality holds:

$$\begin{aligned}(\Upsilon_1+\Upsilon_2\Upsilon_3\Upsilon_4)^{-1} = \Upsilon_1^{-1}-\Upsilon_1^{-1}\Upsilon_2(\Upsilon_3^{-1}\\ +\Upsilon_4\Upsilon_1^{-1}\Upsilon_2)^{-1}\Upsilon_4\Upsilon_1^{-1}.\end{aligned}$$

Based on Proposition 2 and Lemma 2, a key inequality used in the boundedness analysis is given as follows.

Lemma 3: Consider matrix $E(k)$ output by Algorithm 1. Let $\tilde{E}(k) \triangleq E(k)E^T(k)$. Then, the following matrix inequality holds when $t\in\mathbb{N}_+$:

$$\begin{aligned}&\tilde{E}^{-1}(\bar{k}_{t+1})\\ &\ge \bar{\sigma}^{-1}\mathscr{A}^{-T}(\bar{k}_{t+1},\bar{k}_t)\tilde{E}^{-1}(\bar{k}_t)\mathscr{A}^{-1}(\bar{k}_{t+1},\bar{k}_t)\\ &\quad+\bar{\sigma}^{-1}\mathscr{A}^{-T}(\bar{k}_{t+1},\bar{k}_t)\mathcal{C}^T(\bar{k}_{t+1})\Phi^{-1}(\bar{k}_{t+1})\mathcal{C}(\bar{k}_{t+1})\\ &\qquad\times\mathscr{A}^{-1}(\bar{k}_{t+1},\bar{k}_t)\end{aligned}\tag{44}$$

where $\bar{\sigma}\triangleq 1+\sigma^{-1}$ and $\sigma\triangleq\underline{a}\bar{b}^{-1}(\underline{b}^{-1}+\underline{v}^{-1}\bar{c})^{-1}$.

Proof: From the proof of Theorem 3, it can be seen that matrix $E(\bar{k}_{t+1})$ output by Algorithm 1 satisfies

$$\begin{aligned}&\tilde{E}(\bar{k}_{t+1})\\ &=\mathscr{A}(\bar{k}_{t+1},\bar{k}_t)\tilde{E}(\bar{k}_t)\mathscr{A}^T(\bar{k}_{t+1},\bar{k}_t)\\ &\quad-\mathscr{A}(\bar{k}_{t+1},\bar{k}_t)\tilde{E}(\bar{k}_t)\mathcal{C}^T(\bar{k}_{t+1})\\ &\quad\times\Gamma^{-1}(\bar{k}_{t+1})\mathcal{C}(\bar{k}_{t+1})\tilde{E}(\bar{k}_t)\mathscr{A}^T(\bar{k}_{t+1},\bar{k}_t)\\ &\quad+\mathscr{B}(\bar{k}_{t+1},\bar{k}_t)\mathbf{W}(\bar{k}_{t+1})\mathbf{W}^T(\bar{k}_{t+1})\mathscr{B}^T(\bar{k}_{t+1},\bar{k}_t).\end{aligned}\tag{45}$$

Applying Lemma 2 to (45) gives

$$\begin{aligned}&\tilde{E}(\bar{k}_{t+1})\\ &=\Big(\mathscr{A}^{-T}(\bar{k}_{t+1},\bar{k}_t)\tilde{E}^{-1}(\bar{k}_t)\mathscr{A}^{-1}(\bar{k}_{t+1},\bar{k}_t)+\mathscr{A}^{-T}(\bar{k}_{t+1},\bar{k}_t)\\ &\quad\times\mathcal{C}^T(\bar{k}_{t+1})\Phi^{-1}(\bar{k}_{t+1})\mathcal{C}(\bar{k}_{t+1})\mathscr{A}^{-1}(\bar{k}_{t+1},\bar{k}_t)\Big)^{-1}\\ &\quad+\mathscr{B}(\bar{k}_{t+1},\bar{k}_t)\mathbf{W}(\bar{k}_{t+1})\mathbf{W}^T(\bar{k}_{t+1})\mathscr{B}^T(\bar{k}_{t+1},\bar{k}_t).\end{aligned}\tag{46}$$

From (46) and Proposition 2, it is easy to see that

$$\begin{aligned}\tilde{E}(\bar{k}_{t+1}) &\ge \mathscr{B}(\bar{k}_{t+1},\bar{k}_t)\mathbf{W}(\bar{k}_{t+1})\mathbf{W}^T(\bar{k}_{t+1})\mathscr{B}^T(\bar{k}_{t+1},\bar{k}_t)\\ &\ge \underline{b}I,\ \forall t\in\mathbb{N}_+\end{aligned}\tag{47}$$

which also guarantees the invertibility of $\tilde{E}(\bar{k}_{t+1})$. With (47) and Proposition 2, it can be deduced that

$$\begin{aligned}&\mathscr{A}^{-T}(\bar{k}_{t+1},\bar{k}_t)\tilde{E}^{-1}(\bar{k}_t)\mathscr{A}^{-1}(\bar{k}_{t+1},\bar{k}_t)\\ &+\mathscr{A}^{-T}(\bar{k}_{t+1},\bar{k}_t)\mathcal{C}^T(\bar{k}_{t+1})\Phi^{-1}(\bar{k}_{t+1})\mathcal{C}(\bar{k}_{t+1})\mathscr{A}^{-1}(\bar{k}_{t+1},\bar{k}_t)\\ &<\underline{a}^{-1}\underline{b}^{-1}I+\underline{v}^{-1}\underline{a}^{-1}\bar{c}I\end{aligned}\tag{48}$$

where the following relationships

$$\begin{aligned}\Phi_i(\bar{k}_{t+1}) &= \mathscr{D}_i(\bar{k}_{t+1})\vec{\mathbf{W}}_i(\bar{k}_{t+1})\vec{\mathbf{W}}_i^T(\bar{k}_{t+1})\mathscr{D}_i^T(\bar{k}_{t+1})\\ &\quad+\vec{V}_i(\bar{k}_{t+1})\vec{V}_i^T(\bar{k}_{t+1})>\underline{v}I\\ \Phi(\bar{k}_{t+1}) &= \mathrm{diag}_{i\in\mathscr{I}(\bar{k}_{t+1})}^N\{\Phi_i(\bar{k}_{t+1})\}>\underline{v}I\end{aligned}$$

are used. In view of (48), it can be derived that

$$\begin{aligned}&\Big(\mathscr{A}^{-T}(\bar{k}_{t+1},\bar{k}_t)\tilde{E}^{-1}(\bar{k}_t)\mathscr{A}^{-1}(\bar{k}_{t+1},\bar{k}_t)+\mathscr{A}^{-T}(\bar{k}_{t+1},\bar{k}_t)\\ &\quad\times\mathcal{C}^T(\bar{k}_{t+1})\Phi^{-1}(\bar{k}_{t+1})\mathcal{C}(\bar{k}_{t+1})\mathscr{A}^{-1}(\bar{k}_{t+1},\bar{k}_t)\Big)^{-1}\\ &>\underline{a}(\underline{b}^{-1}+\underline{v}^{-1}\bar{c})^{-1}I\\ &=\sigma\bar{b}I\\ &>\sigma\mathscr{B}(\bar{k}_{t+1},\bar{k}_t)\mathbf{W}(\bar{k}_{t+1})\mathbf{W}^T(\bar{k}_{t+1})\mathscr{B}^T(\bar{k}_{t+1},\bar{k}_t).\end{aligned}\tag{49}$$

According to (46) and (49), it follows that

$$\begin{aligned}&\tilde{E}(\bar{k}_{t+1})\\ &\le\bar{\sigma}\Big(\mathscr{A}^{-T}(\bar{k}_{t+1},\bar{k}_t)\tilde{E}^{-1}(\bar{k}_t)\mathscr{A}^{-1}(\bar{k}_{t+1},\bar{k}_t)+\mathscr{A}^{-T}(\bar{k}_{t+1},\bar{k}_t)\\ &\quad\times\mathcal{C}^T(\bar{k}_{t+1})\Phi^{-1}(\bar{k}_{t+1})\mathcal{C}(\bar{k}_{t+1})\mathscr{A}^{-1}(\bar{k}_{t+1},\bar{k}_t)\Big)^{-1}\end{aligned}$$

which further gives (44). The proof is complete. ∎

In the following theorem, the uniform upper bound of the F-radius of the zonotope output by Algorithm 1 is given based on Lemma 3.

Theorem 6: Assume that there exist a positive scalar $\bar{e}$ and a positive integer z such that the following matrix inequalities hold:

$$\begin{aligned}&\sum_{\ell=t+1-z}^{t+1}\bar{\sigma}^{-(t+2-\ell)}\mathscr{A}^{-T}(\bar{k}_{t+1},\bar{k}_t)\cdots\mathscr{A}^{-T}(\bar{k}_\ell,\bar{k}_{\ell-1})\mathcal{C}^T(\bar{k}_\ell)\\ &\quad\times\Phi^{-1}(\bar{k}_\ell)\mathcal{C}(\bar{k}_\ell)\mathscr{A}^{-1}(\bar{k}_\ell,\bar{k}_{\ell-1})\cdots\mathscr{A}^{-1}(\bar{k}_{t+1},\bar{k}_t)\\ &>\bar{e}^{-1}I,\quad\text{when } t\ge z-1\end{aligned}\tag{50}$$

$$\tilde{E}(\bar{k}_t)<\bar{e}I,\ \text{when } t\in\{0,1,\ldots,z-1\}.\tag{51}$$

Then, $\tilde{E}(\bar{k}_t)$ is upper bounded by $\bar{e}I$ for all $t\in\mathbb{N}$, that is,

$$\tilde{E}(\bar{k}_t)<\bar{e}I.\tag{52}$$

In addition, for any time instant $k\in\mathbb{N}$, one has

$$\tilde{E}(k)<\vec{e}I\tag{53}$$

where $\vec{e}\triangleq\bar{e}(\max\{1,\bar{\alpha}\})^{\vec{\eta}}+\bar{\beta}(1+\bar{\alpha}+\cdots+\bar{\alpha}^{\vec{\eta}-1})$, and $\vec{\eta}$ has been defined in the proof of Proposition 2. Furthermore,

the F-radius of the zonotope output by Algorithm 1 is upper bounded by $\sqrt{\vec{e}nN}$, that is,

$$\|E(k)\|_F \leq \sqrt{\vec{e}nN},\ \forall k \in \mathbb{N}. \tag{54}$$

Proof: By iterating the matrix inequality in (44) for z times, we obtain that

$$\begin{aligned}
&\tilde{E}^{-1}(\bar{k}_{t+1})\\
&\geq \bar{\sigma}^{-(z+1)}\mathscr{A}^{-T}(\bar{k}_{t+1},\bar{k}_t)\cdots\mathscr{A}^{-T}(\bar{k}_{t-z+1},\bar{k}_{t-z})\tilde{E}^{-1}(\bar{k}_{t-z})\\
&\quad\times\mathscr{A}^{-1}(\bar{k}_{t-z+1},\bar{k}_{t-z})\cdots\mathscr{A}^{-1}(\bar{k}_{t+1},\bar{k}_t)\\
&\quad+\sum_{\ell=t+1-z}^{t+1}\bar{\sigma}^{-(t+2-\ell)}\mathscr{A}^{-T}(\bar{k}_{t+1},\bar{k}_t)\cdots\mathscr{A}^{-T}(\bar{k}_\ell,\bar{k}_{\ell-1})\\
&\quad\times\mathcal{C}^T(\bar{k}_\ell)\Phi^{-1}(\bar{k}_\ell)\mathcal{C}(\bar{k}_\ell)\mathscr{A}^{-1}(\bar{k}_\ell,\bar{k}_{\ell-1})\cdots\mathscr{A}^{-1}(\bar{k}_{t+1},\bar{k}_t)\\
&>\sum_{\ell=t+1-z}^{t+1}\bar{\sigma}^{-(t+2-\ell)}\mathscr{A}^{-T}(\bar{k}_{t+1},\bar{k}_t)\cdots\mathscr{A}^{-T}(\bar{k}_\ell,\bar{k}_{\ell-1})\\
&\quad\times\mathcal{C}^T(\bar{k}_\ell)\Phi^{-1}(\bar{k}_\ell)\mathcal{C}(\bar{k}_\ell)\mathscr{A}^{-1}(\bar{k}_\ell,\bar{k}_{\ell-1})\cdots\mathscr{A}^{-1}(\bar{k}_{t+1},\bar{k}_t)
\end{aligned}$$

which, together with (50), implies that (52) holds for $t \in \{z, z+1, \ldots\}$. Furthermore, in view of (51), it follows that (52) holds for all $t \in \mathbb{N}$.

It remains to prove (53). For any $k \notin \{\bar{k}_t\}_{t=0}^{\infty}$, let $k^* \triangleq \max\{k' : k' \in \{\bar{k}_t\}_{t=0}^{\infty}, k' < k\}$. Recalling $\tilde{E}(k) = E(k)E^T(k)$, one can obtain from (17) that

$$\begin{aligned}
\tilde{E}(k) = {}&\mathcal{A}(k-1)E(k-1)E^T(k-1)\mathcal{A}^T(k-1)\\
&+\bar{W}(k-1)\bar{W}^T(k-1).
\end{aligned}$$

By iterating the above equality for $k-k^*-1$ times, one has

$$\begin{aligned}
&\tilde{E}(k)\\
&=\ \mathcal{A}(k-1)\cdots\mathcal{A}(k^*)\tilde{E}(k^*)\mathcal{A}^T(k^*)\cdots\mathcal{A}^T(k-1)\\
&\quad+\bar{W}(k-1)\bar{W}^T(k-1)\\
&\quad+\sum_{\vartheta=2}^{k-k^*}\mathcal{A}(k-1)\cdots\mathcal{A}(k-\vartheta+1)\bar{W}(k-\vartheta)\bar{W}^T(k-\vartheta)\\
&\qquad\times\mathcal{A}^T(k-\vartheta+1)\cdots\mathcal{A}^T(k-1).
\end{aligned}\tag{55}$$

Applying (52) and Assumption 2 to (55), one can readily obtain

$$\begin{aligned}
\tilde{E}(k) &< \bar{e}\bar{\alpha}^{k-k^*}I+\bar{\beta}(1+\bar{\alpha}+\cdots+\bar{\alpha}^{k-k^*-1})I\\
&\leq \bar{e}(\max\{1,\bar{\alpha}\})^{\vec{\eta}}I+\bar{\beta}(1+\bar{\alpha}+\cdots+\bar{\alpha}^{\vec{\eta}-1})I\\
&= \vec{e}I.
\end{aligned}$$

When $k \in \{\bar{k}_t\}_{t=0}^{\infty}$, due to $\bar{e} < \vec{e}$, it can be seen from (52) that (53) still holds, which means that (53) is satisfied for any time instant $k \in \mathbb{N}$. Finally, it follows from (53) that

$$\|E(k)\|_F = \sqrt{\mathrm{Tr}\{\tilde{E}(k)\}} < \sqrt{\mathrm{Tr}\{\vec{e}I\}} = \sqrt{\vec{e}nN},$$

which ends the proof. ∎

In the following, we proceed to analyze the uniform boundedness of the F-radius of the zonotope output by Algorithm 2.

Theorem 7: Assume that there exist a positive scalar $\bar{e}$ and a positive integer z such that matrix inequalities (50) and (51) hold for all $t \in \mathbb{N}$. Then, the F-radius of the zonotope output by Algorithm 2 is upper bounded by $\sqrt{\vec{e}nN}$, that is,

$$\|\check{E}(k)\|_F \leq \sqrt{\vec{e}nN},\ \forall k \in \mathbb{N}. \tag{56}$$

Proof: From the initialization of Algorithms 1 and 2, it can be seen that $\tilde{E}(0) = \check{E}(0)\check{E}^T(0)$. Assume that $\tilde{E}(k) = \check{E}(k)\check{E}^T(k)$ holds. In the following, we will show that $\tilde{E}(k+1) = \check{E}(k+1)\check{E}^T(k+1)$ also holds. When $k+1 \notin \{\bar{k}_t\}_{t=1}^{\infty}$, one can derive from (17) and (36) that $\tilde{E}(k+1) = \check{E}(k+1)\check{E}^T(k+1)$. Otherwise, there exists an integer $t \in \mathbb{N}$ such that $k+1 = \bar{k}_{t+1}$. In this case, similar to (45), one can see that the matrix $\check{E}(\bar{k}_{t+1})$ output by Algorithm 2 satisfies

$$\begin{aligned}
&\check{E}(\bar{k}_{t+1})\check{E}^T(\bar{k}_{t+1})\\
&=\mathscr{A}(\bar{k}_{t+1},\bar{k}_t)\check{E}(\bar{k}_t)\check{E}^T(\bar{k}_t)\mathscr{A}^T(\bar{k}_{t+1},\bar{k}_t)\\
&\quad+\mathscr{B}(\bar{k}_{t+1},\bar{k}_t)\mathbf{W}(\bar{k}_{t+1})\mathbf{W}^T(\bar{k}_{t+1})\mathscr{B}^T(\bar{k}_{t+1},\bar{k}_t)\\
&\quad-\mathscr{A}(\bar{k}_{t+1},\bar{k}_t)\check{E}(\bar{k}_t)\check{E}^T(\bar{k}_t)\mathcal{H}^T(\bar{k}_{t+1})\check{\Gamma}^{-1}(\bar{k}_{t+1})\\
&\quad\times\mathcal{H}(\bar{k}_{t+1})\check{E}(\bar{k}_t)\check{E}^T(\bar{k}_t)\mathscr{A}^T(\bar{k}_{t+1},\bar{k}_t).
\end{aligned}\tag{57}$$

Then, applying Lemma 2 to (57) yields

$$\begin{aligned}
&\check{E}(\bar{k}_{t+1})\check{E}^T(\bar{k}_{t+1})\\
&=\Big(\mathscr{A}^{-T}(\bar{k}_{t+1},\bar{k}_t)(\check{E}(\bar{k}_t)\check{E}^T(\bar{k}_t))^{-1}\mathscr{A}^{-1}(\bar{k}_{t+1},\bar{k}_t)\\
&\quad+\mathscr{A}^{-T}(\bar{k}_{t+1},\bar{k}_t)\mathcal{H}^T(\bar{k}_{t+1})(\widehat{\varepsilon}(\bar{k}_{t+1})\widehat{\varepsilon}^T(\bar{k}_{t+1}))^{-1}\\
&\qquad\times\mathcal{H}(\bar{k}_{t+1})\mathscr{A}^{-1}(\bar{k}_{t+1},\bar{k}_t)\Big)^{-1}\\
&\quad+\mathscr{B}(\bar{k}_{t+1},\bar{k}_t)\mathbf{W}(\bar{k}_{t+1})\mathbf{W}^T(\bar{k}_{t+1})\mathscr{B}^T(\bar{k}_{t+1},\bar{k}_t).
\end{aligned}\tag{58}$$

Substituting the expression of $\widehat{\varepsilon}(\bar{k}_{t+1})$ (below (32)) to (58) and observing (33) and (46), it can be found that

$$\tilde{E}(\bar{k}_{t+1}) = \check{E}(\bar{k}_{t+1})\check{E}^T(\bar{k}_{t+1}).$$

Therefore, $\tilde{E}(k) = \check{E}(k)\check{E}^T(k)$ holds for all $k \in \mathbb{N}$, which gives $\mathrm{Tr}\{\tilde{E}(k)\} = \mathrm{Tr}\{\check{E}(k)\check{E}^T(k)\}$. In other words, the zonotopes output by Algorithms 1 and 2 have the same F-radius. Keeping this fact in mind, it can be seen from Theorem 6 that the result of this theorem is also true. ∎

Remark 6: Under a commonly utilized assumption in the steady-state performance analysis for time-varying systems (i.e., Assumption 2), two sufficient criteria are established to ensure the steady-state performance of the proposed SMFE algorithms, where Theorem 6 guarantees the performance of the parallel fusion estimation algorithm, and Theorem 7 ascertains the performance of the data compression fusion estimation algorithm. Although the obtained uniform upper bounds in Theorems 6 and 7 may be relatively large, their existence prevents divergence in both the parallel fusion estimation algorithm and the data compression fusion estimation algorithm. Note that both the estimator under the parallel fusion scheme in (14)–(15) and the estimator under the data compression fusion scheme in (34)–(35) are essentially one-step predictors. Therefore, the existed uniform boundedness analysis methods for Kalman-type estimators in [27] cannot be directly used. To obtain the desired criteria, a fundamental difficulty is to derive the relationship between $\tilde{E}^{-1}(\bar{k}_{t+1})$ and $\tilde{E}^{-1}(\bar{k}_t)$. Such a challenge is solved in Lemma 3. Details can be seen in the proof of this lemma.

Remark 7: In this paper, the buffer-aided strategy is adopted with the aim of improving estimation performance. From $\kappa_{i,t'} \triangleq \min\{M_i, \Delta\eta_{i,t'}\}$ and $\iota_{i,t+1} = \min\{\kappa_{i,t'}, \Delta\bar{k}_{t+1}\}$, it

can be verified that $\iota_{i,t+1}$ is nondecreasing with respect to the buffer capacity M_i. Furthermore, according to (46) and

$$\begin{aligned}&\mathcal{C}^T(\bar{k}_{t+1})\Phi^{-1}(\bar{k}_{t+1})\mathcal{C}(\bar{k}_{t+1})\\&=\sum_{i\in\mathscr{I}(\bar{k}_{t+1})}\sum_{s=1}^{\iota_{i,t+1}}\mathscr{A}^T(\bar{k}_{t+1}+1-s,\bar{k}_t)\bar{C}_i^T(\bar{k}_{t+1}+1-s)\\&\quad\times\underline{\Phi}_i^{-1}(\bar{k}_{t+1}+1-s,\bar{k}_t)\bar{C}_i(\bar{k}_{t+1}+1-s)\\&\quad\times\mathscr{A}(\bar{k}_{t+1}+1-s,\bar{k}_t)\end{aligned}$$

it follows that $\mathrm{Tr}\{\tilde{E}(\bar{k}_{t+1})\}$ does not increase with increasing M_i. Moreover, it can be shown that, within a certain range, a larger M_i facilitates the satisfaction of the inequality in (50).

Remark 8: Up to now, the zonotopic SMFE issue for CNs has been addressed using a buffer-aided strategy. Compared with the existing literature, the following key differences distinguish the present work.

1) A novel batch processing approach has been proposed to process and utilize the data from the buffers of the considered CN. Unlike conventional re-estimation methods that require multiple iterations, the proposed batch processing method allows buffered data to be employed collectively in a unified framework. This significantly simplifies the design procedure of the estimation algorithms and facilitates a more efficient use of measurement information.
2) Two centralized SMFE algorithms have been designed, which are respectively based on the parallel fusion scheme and the data compression scheme. Both algorithms have been structured in a recursive manner, enabling their straightforward application in real-time or online estimation scenarios. Moreover, the data compression fusion scheme offers computational efficiency while maintaining the estimation performance comparable to the parallel fusion scheme.
3) Sufficient criteria, which are applicable to CNs exhibiting instability, have been rigorously established to guarantee the uniform boundedness of the estimation error zonotopes and the steady-state performance of the proposed SMFE algorithms. This ensures the robustness and reliability of the algorithms even under challenging operating conditions.

IV. ILLUSTRATIVE EXAMPLES

In this section, two examples of CNs are employed to show the utility of the proposed zonotopic SMFE algorithms.

Example 1. Consider a CN composed of 8 nodes with the dynamics of the i-th node being given as follows:

$$\begin{cases}x_i(k+1)=\begin{bmatrix}1.02+0.1\cos(k) & 0 & 0\\ 0 & 0.5 & 0.2\\ 0.3\cos(k) & 0 & 0.1\end{bmatrix}x_i(k)+w_i(k)\\ \qquad\qquad+\sum_{j=1}^{N}\lambda_{ij}(k)\mathrm{diag}\{0.1,0.2,0.3\}x_j(k)\\ y_i(k)=\begin{bmatrix}1&0&0\\0&1&0\end{bmatrix}x_i(k)+v_i(k)\end{cases}$$

where

$$\Lambda(k)=\begin{cases}\begin{bmatrix}0&0.1&0.1&0&0&0&0&0\\0&0&0.1&0.1&0&0&0&0\\0&0&0&0.1&0.1&0&0&0\\0&0&0&0&0.1&0.1&0&0\\0&0&0&0&0&0.1&0.1&0\\0&0&0&0&0&0&0.1&0.1\\0.1&0&0&0&0&0&0&0.1\\0.1&0.1&0&0&0&0&0&0\end{bmatrix},\text{if } \mathrm{mod}(k,2)=0\\ \begin{bmatrix}0&0&0.1&0&0&0&0&0\\0&0&0&0.1&0&0&0&0\\0&0&0&0&0.1&0&0&0\\0&0&0&0&0&0.1&0&0\\0&0&0&0&0&0&0.1&0\\0&0&0&0&0&0&0&0.1\\0.1&0&0&0&0&0&0&0\\0&0.1&0&0&0&0&0&0\end{bmatrix},\text{otherwise}\end{cases}$$

all components of the noises $w_i(k)$ and $v_i(k)$ $(i=1,2,\ldots,5)$ are all drawn from a uniform distribution on $[-0.2,0.2]$; the initial state $\mathbf{x}(0)$ is set to be $\mathbf{x}(0)=0.1\mathrm{vec}_{24}\{1\}$. Correspondingly, for $i=1,2,\ldots,8$, parameters $W_i(k)$, $V_i(k)$, and $X_i(k)$ are selected as $0.2I_3$, $0.2I_2$, and $0.2I_3$, respectively.

For the considered CN, the parameters of the equipped buffers are given as follows:

$$\begin{aligned}\begin{bmatrix}M_1&M_2&\cdots&M_8\end{bmatrix}&=\begin{bmatrix}2&2&3&3&4&4&4&4\end{bmatrix}\\ \begin{bmatrix}\bar{\eta}_1&\bar{\eta}_2&\cdots&\bar{\eta}_8\end{bmatrix}&=\begin{bmatrix}3&3&3&4&4&5&5&5\end{bmatrix}.\end{aligned}$$

The transmission moments and transmission intervals of the buffers are depicted in Figs. 1 and 2, respectively.

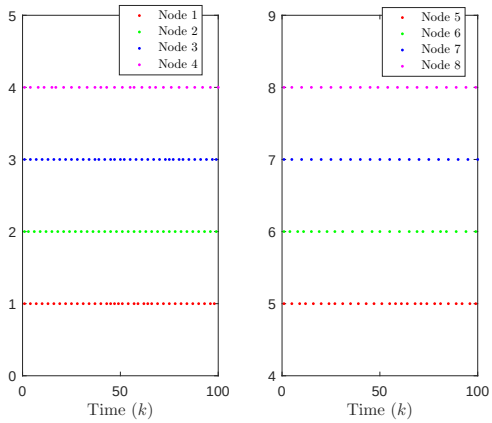

Fig. 1: Transmission time instants of the buffers.

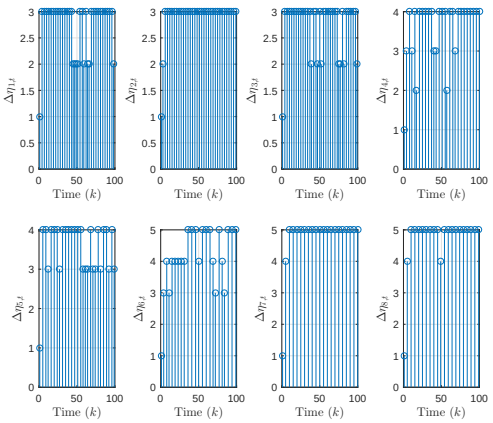

Fig. 2: Transmission intervals of the buffers.

Firstly, we examine effectiveness of the proposed parallel fusion estimation algorithm (i.e., Algorithm 1). Fig. 3 depicts

the estimation performance of partial state variables, where $\mathbf{x}^{(\cdot)}(k)$ and $\hat{x}^{(\cdot)}(k)$ denote certain components of $\mathbf{x}(k)$ and $\hat{x}(k)$, respectively, and the bounds are calculated by $\hat{x}(k) \pm \mathrm{rs}\{E(k)\}\mathbf{1}$. From this figure, we can see that Algorithm 1 performs well. Moreover, to show the role of the buffer-aided strategy, Fig. 4 gives the information about the F-radius of zonotope $\langle 0, E(k)\rangle$ output by Algorithm 1 with and without the buffer-aided strategy, respectively. The corresponding average F-radii (defined as $(1/100)\sum_{k=1}^{100}\|E(k)\|_F$) are 1.4532 and 1.4687, respectively. It is clear that the usage of the buffer-aided strategy can effectively improve the estimation performance.

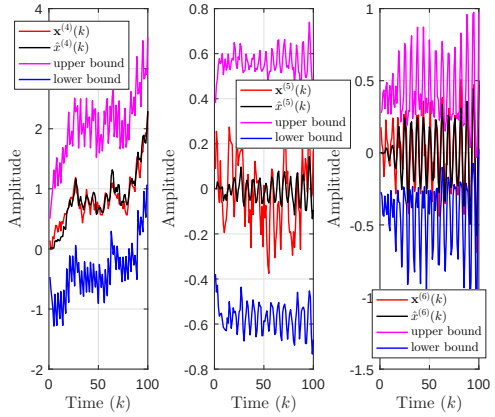

Fig. 3: Partial state variables of $\mathbf{x}(k)$, their estimates output by Algorithm 1, and the corresponding upper/lower bounds.

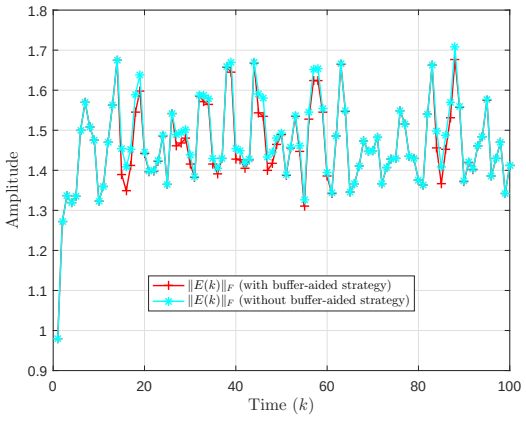

Fig. 4: $\|E(k)\|_F$ with and without the buffer-aided strategy.

In the following, let us check the performance of the designed data compression fusion estimator. The estimation performance with Algorithm 2 is provided in Fig. 5, where $\check{x}^{(\cdot)}(k)$ represents certain component of $\check{x}(k)$. It can be observed that the estimation performance of Algorithm 2 is as good as that of Algorithm 1.

To further validate the effectiveness of the proposed SMFE method, it is compared with the ellipsoidal SME method in [12], [41], [46]. Fig. 6 presents the 2-norm of the estimation error over time, indicating that the proposed method achieves superior performance.

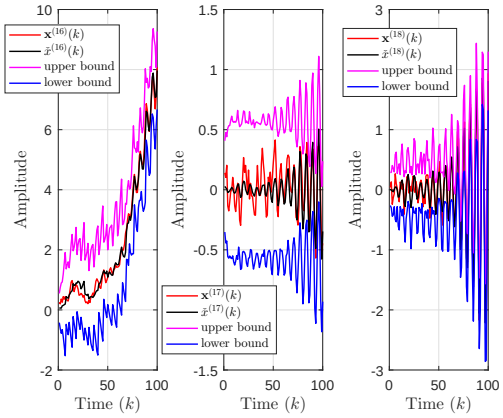

Fig. 5: Partial state variables of $\mathbf{x}(k)$, their estimates output by Algorithm 2, and the corresponding upper/lower bounds.

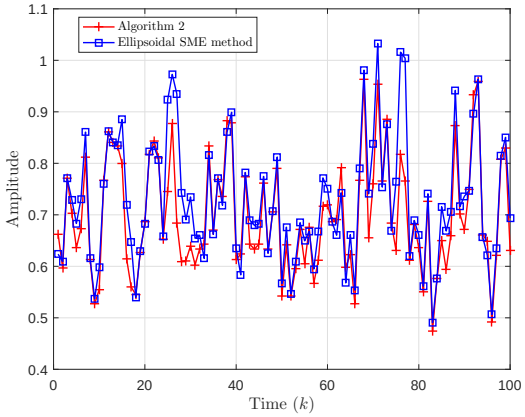

Fig. 6: 2-norm of estimation error under Algorithm 2 and the ellipsoidal SME method in [12], [41], [46].

Example 2. In this example, the feasibility of the results regarding the uniform boundedness analysis will be confirmed.

Consider the following CN with $N = 3$:

$$\begin{cases} x_i(k+1) = \mathrm{diag}\{1.02, 0.5\}x_i(k) + w_i(k) \\ \qquad\qquad + \sum_{j=1}^{N} \lambda_{ij}(k)\mathrm{diag}\{0.1, 0.2\}x_j(k) \\ y_1(k) = (0.9 + 0.1\sin(0.1k)) \begin{bmatrix} 1 & 0 \end{bmatrix} x_1(k) + v_1(k) \\ y_2(k) = (0.9 + 0.1\cos(0.2k)) \begin{bmatrix} 1 & 0 \end{bmatrix} x_2(k) + v_2(k) \\ y_3(k) = (0.9 + 0.1\sin(0.3k)) \begin{bmatrix} 0 & 1 \end{bmatrix} x_3(k) + v_3(k) \\ x_i(0) = \begin{bmatrix} 0.1 & 0.1 \end{bmatrix}^T \end{cases}$$

where

$$\Lambda(k) = \begin{bmatrix} 0 & 0.1 & 0.1 \\ 0 & 0 & 0.2 \\ 0.2 & 0 & 0 \end{bmatrix}$$

and, for $i = 1, 2, 3$, $w_i(k) = \begin{bmatrix} 0.1\cos(k) & 0.1\cos(k) \end{bmatrix}^T$ and $v_i(k) = 0.1\sin(k)$.

In this example, parameters $W_i(k)$, $V_i(k)$, and $X_i(k)$ $(i = 1, 2, 3)$ are selected as $0.1I_2$, 0.1, and $0.1I_2$, respectively.

Moreover, for convenience, the buffers' parameters are set as $M_i = 2$, $\eta_{i,1} = 1$, and $\Delta\eta_{i,t} = 3$ for $i = 1, 2, 3$.

With the above parameters and $\underline{\alpha} = 0.2195$, $\bar{\alpha} = 1.0828$, $\underline{\beta} = 0.01$, $\bar{\beta} = 0.01$, $\bar{\gamma} = 0.996$, and $\underline{v} = 0.01$, we can confirm that Assumption 2 holds. Then, according to the proof of Proposition 2, we have $\vec{\eta} = 3$, $\underline{a} = 0.0105$, $\bar{a} = 1.27$, $\underline{b} = 0.01$, $\bar{b} = 0.0354$, $\bar{c} = 11.38$, and $\bar{\sigma} = 4.142 \times 10^3$. Furthermore, we can see that, with $\bar{e} = 1.4964 \times 10^{21}$ and $z = 2$, condition (50) is satisfied, and $\vec{e}$ can be calculated as 1.9484×10^{21}. With the calculated $\vec{e}$, the information about $\|E(k)\|_F$, $\|\check{E}(k)\|_F$, as well as their uniform upper bounds in (54) and (56) is presented in Fig. 7, which shows the validity of Theorems 6 and 7. Moreover, the state estimation performance of Algorithms 1 and 2 are illustrated in Figs. 8 and 9. It can be seen that both the proposed parallel fusion estimation algorithm and the data compression estimation algorithm can achieve an ideal estimation performance.

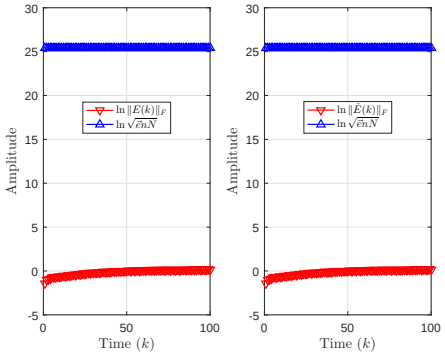

Fig. 7: $\|E(k)\|_F$, $\|\check{E}(k)\|_F$, and their uniform upper bounds.

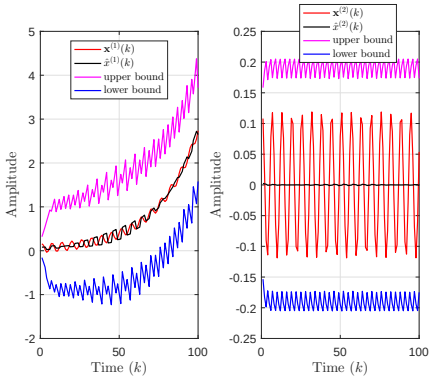

Fig. 8: Partial state variables of $\mathbf{x}(k)$, their estimates output by Algorithm 1, and the upper/lower bounds.

V. CONCLUSION

In this paper, the buffer-aided zonotopic SMFE problem for CNs has been investigated. Each node of the CN has been equipped with a buffer for real-time data storage, enabling the fusion center to utilize additional measurement information when the node's transmission interval exceeds its sampling period. A batch processing method has been proposed to efficiently process the data received at the fusion center. By employing the zonotopic SME technique, two

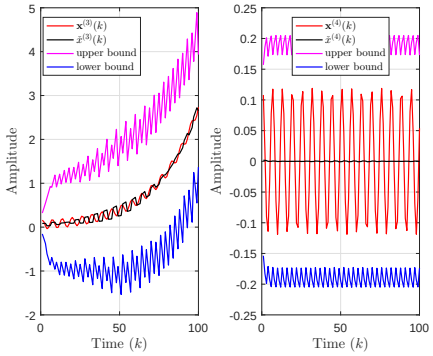

Fig. 9: Partial state variables of $\mathbf{x}(k)$, their estimates output by Algorithm 2, and the upper/lower bounds.

SMFE algorithms have been developed, which are based on the parallel fusion scheme and the data compression fusion scheme, respectively. Furthermore, sufficient conditions have been established to ensure the uniform boundedness of the F-radii of the zonotopes generated by the SMFE algorithms. Future research will focus on extending the proposed SMFE algorithms to CNs with unknown or time-varying topologies, as well as incorporating communication imperfections such as random packet dropouts and delays.

REFERENCES

[1] R. Caballero-Águila, I. García-Garrido, and J. Linares-Pérez, "Information fusion algorithms for state estimation in multi-sensor systems with correlated missing measurements," *Appl. Math. Comput.*, vol. 226, pp. 548–563, 2014.

[2] R. Caballero-Águila, A. Hermoso-Carazo, and J. Linares-Pérez, "Centralized, distributed and sequential fusion estimation from uncertain outputs with correlation between sensor noises and signal," *Int. J. Gener. Syst.*, vol. 48, no. 7, pp. 713–737, 2019.

[3] R. Caballero-Águila and J. Linares-Pérez, "Centralized fusion estimation in networked systems: Addressing deception attacks and packet dropouts with a zero-order hold approach," *Int. J. Netw. Dyn. Intell.*, vol. 3, no. 4, art. no. 100021, 2024.

[4] H. Chen, Q. Chen, B. Shen, and Y. Liu, "Parameter learning of probabilistic Boolean control networks with input-output data," *Int. J. Netw. Dyn. Intell.*, vol. 3, no. 1, art. no. 100005, 2024.

[5] C. K. Chui and G. Chen, *Kalman Filtering With Real-Time Applications*, 4th ed. Berlin, Heidelberg, Germany: Springer, 2009.

[6] C. Combastel, "Zonotopes and Kalman observers: Gain optimality under distinct uncertainty paradigms and robust convergence," *Automatica*, vol. 55, pp. 265–273, 2015.

[7] C. Deng, C. Wen, W. Wang, X. Li, and D. Yue, "Distributed adaptive tracking control for high-order nonlinear multiagent systems over event-triggered communication," *IEEE Trans. Autom. Control*, vol. 68, no. 2, pp. 1176–1183, Feb. 2023.

[8] X. Du, L. Zou, and M. Zhong, "Set-membership filtering approach to dynamic event-triggered fault estimation for a class of nonlinear time-varying complex networks, *IEEE/CAA J. Autom. Sinica*, vol. 11, no. 3, pp. 638–648, Mar. 2024.

[9] Z. Fei, Y. Liu, X.-M. Sun, and S. Ren, "Zonotopic set-membership state estimation for switched systems with restricted switching," *IEEE Trans. Autom. Control*, vol. 67, no. 11, pp. 6127–6134, Nov. 2022.

[10] P. Gao, C. Jia, and A. Zhou, "Encryption-decryption-based state estimation for nonlinear complex networks subject to coupled perturbation," *Syst. Sci. Control Eng.*, vol. 12, no. 1, art. no. 2357796, 2024.

[11] X. Gao, F. Deng, W. Shang, X. Zhao, and S. Li, "Attack-resilient asynchronous state estimation of interval type-2 fuzzy systems under stochastic protocols," *Int. J. Syst. Sci.*, vol. 55, no. 13, pp. 2688–2700, 2024.

[12] X. Ge, Q.-L. Han, and Z. Wang, "A dynamic event-triggered transmission scheme for distributed set-membership estimation over wireless sensor networks," *IEEE Trans. Cybern.*, vol. 49, no. 1, pp. 171–183, Jan. 2019.

[13] Y. Guo, Z. Wang, J.-Y. Li, and Y. Xu, "An impulsive approach to state estimation for multirate singularly perturbed complex networks under bit rate constraints," *IEEE Trans. Cybern.*, vol. 55, no. 3, pp. 1197–1209, Mar. 2025.

[14] Y. Guo, Z. Wang, J.-Y. Li, and Y. Xu, "Pinning synchronization for stochastic complex networks with randomly occurring nonlinearities: tackling bit rate constraints and allocations," *IEEE Trans. Cybern.*, vol. 54, no. 12, pp. 7248–7259, Dec. 2024.

[15] G. Hao, S.-L. Sun, and Y. Li, "Nonlinear weighted measurement fusion unscented Kalman filter with asymptotic optimality," *Inf. Sci.*, vol. 299, pp. 85–98, 2015.

[16] H. V. Henderson and S. R. Searle, "On deriving the inverse of a sum of matrices," *SIAM Rev.*, vol. 23, no. 1, pp. 53–60, 1981.

[17] C. Hu, S. Ding, and X. Xie, "Event-based distributed set-membership estimation for complex networks under deception attacks," *IEEE Trans. Automa. Sci. Eng.*, vol. 21, no. 3, pp. 3719–3729, Jul. 2024.

[18] C. Hu, X. Xie, S. Ding, and Y. Jing, "Distributed set-membership fusion estimation for complex networks with communication constraints," *IEEE Trans. Automa. Sci. Eng.*, vol. 22, pp. 3877–3886, 2025.

[19] L. Hu, Y. Yang, Z. Tang, Y. He, and X. Luo, "FCAN-MOPSO: An improved fuzzy-based graph clustering algorithm for complex networks with multi-objective particle swarm optimization," *IEEE Trans. Fuzzy Syst.*, vol. 31, no. 10, pp. 3470–3484, Oct. 2023.

[20] S. Hu, X. Ge, W. Zhang, and D. Yue, "DoS-resilient load frequency control of multi-area power systems: An attack-parameter-dependent approach," *IEEE Trans. Inf. Forensics Security*, vol. 19, pp. 3423–3434, 2024.

[21] C. Jia, J. Hu, X. Yi, H. Liu, J. Huang, and Z. Cao, "Recursive state estimation for a class of quantized coupled complex networks subject to missing measurements and amplify-and-forward relay," *Inf. Sci.*, vol. 630, pp. 53–73, 2023.

[22] F. Jin, L. Ma, C. Zhao, and Q. Liu, "State estimation in networked control systems with a real-time transport protocol," *Syst. Sci. Control Eng.*, vol. 12, no. 1, art. no. 2347885, 2024.

[23] W. Kühn, "Rigorously computed orbits of dynamical systems without the wrapping effect," *Computing*, vol. 61, pp. 47–67, 1998.

[24] V. T. H. Le, C. Stoica, T. Alamo, E. F. Camacho, and D. Dumur, *Zonotopes: From Guaranteed State-estimation to Control*, ISTE Ltd, 2013.

[25] B. Lei, J. Hu, R. Caballero-Águila, and C. Chen, "Hybrid-attack-resistant distributed state estimation for nonlinear complex networks with random coupling strength and sensor delays," *J. Frankl. Inst.*, vol. 361, no. 13, art. no. 107005, 2024.

[26] C. Li, Y. Liu, M. Gao, and L. Sheng, "Fault-tolerant formation consensus control for time-varying multi-agent systems with stochastic communication protocol," *Int. J. Netw. Dyn. Intell.*, vol. 3, no. 1, art. no. 100004, 2024.

[27] W. Li, G. Wei, D. Ding, Y. Liu, and F. E. Alsaadi, "A new look at boundedness of error covariance of Kalman filtering," *IEEE Trans. Syst., Man, Cybern., Syst.*, vol. 48, no. 2, pp. 309–314, Feb. 2018.

[28] X. R. Li, Y. Zhu, J. Wang, and C. Han, "Optimal linear estimation fusion-Part I: Unified fusion rules," *IEEE Trans. Inf. Theory*, vol. 49, no. 9, pp. 2192–2208, Sep. 2003.

[29] H. Lin and S. Sun, "Globally optimal sequential and distributed fusion state estimation for multi-sensor systems with cross-correlated noises," *Automatica*, vol. 101, pp. 128–137, 2019.

[30] L.-N. Liu and G.-H. Yang, "Distributed energy resource coordination for a microgrid over unreliable communication network with DoS attacks," *Int. J. Syst. Sci.*, vol. 55, no. 2, pp. 237–252, 2024.

[31] S. Liu, P. X. Liu, and A. E. Saddik, "Modeling and stability analysis of automatic generation control over cognitive radio networks in smart grids," *IEEE Trans. Syst., Man, Cybern, Syst.*, vol. 45, no. 2, pp. 223–234, Feb. 2015.

[32] T. Liu, Z. Wang, Y. Liu, and R. Wang, "Unscented-Kalman-filter-based remote state estimation for complex networks with quantized measurements and amplify-and-forward relays," *IEEE Trans. Cybern.*, vol. 54, no. 11, pp. 6819–6831, Nov. 2024.

[33] W.-Q. Liu, X.-M. Wang, and Z.-L. Deng, "Robust centralized and weighted measurement fusion Kalman estimators for uncertain multisensor systems with linearly correlated white noises," *Inf. Fusion*, vol. 35, pp. 11–25, 2017.

[34] X. Meng, Z. Wang, F. Wang, and Y. Chen, "Finite-horizon H_∞ state estimation for complex networks with uncertain couplings and packet losses: Handling amplify-and-forward relays," *IEEE Trans. Neural Netw. Learn. Syst.*, vol. 35, no. 12, pp. 17493–17503, Dec. 2024.

[35] J. Sun, B. Shen, and L. Zou, "Ultimately bounded state estimation for nonlinear networked systems with constrained average bit rate: A buffer-aided strategy," *IEEE Trans. Signal Process.*, vol. 72, pp. 1865–1876, 2024.

[36] H. Tan, B. Shen, Q. Li, and T. Huang, "Zonotopic set-membership estimation for time-varying systems subject to dynamical biases and quantization effects," *Inf. Sci.*, vol. 654, art. no. 119869, 2024.

[37] E. Tian, Y. Zou, and H. Chen, "Finite-time synchronization of complex networks with intermittent couplings and neutral-type delays," *IEEE/CAA J. Autom. Sinica*, vol. 10, no. 10, pp. 2026–2028, Oct. 2023.

[38] B. Xu, J. Hu, X. Yi, D. Chen, H. Yu, and Z. Wu, "Minimum-variance recursive state estimation for complex networks with stochastic switching topologies and random quantization under try-once-discard protocol," *Int. J. Robust Nonlinear Control*, vol. 37, no. 1, pp. 105–125, 2023.

[39] C. Xu, H. Dong, Y. Shen, and J. Li, "Dynamic event-triggered fault estimation for complex networks with time-correlated fading channels," *Inf. Sci.*, vol. 644, art. no. 119288, 2023.

[40] Y. Xu, L. Yang, Z. Wang, H. Rao, and R. Lu, "State estimation for networked systems with Markov driven transmission and buffer constraint," *IEEE Trans. Syst., Man, Cybern., Syst.*, vol. 51, no. 12, pp. 7727–7734, Dec. 2021.

[41] B. Yang, Q. Qiu, Q.-L. Han, and F. Yang, "Received signal strength indicator-based indoor localization using distributed set-membership filtering," *IEEE Trans. Cybern.*, vol. 52, no. 2, pp. 727–737, Feb. 2022.

[42] H. Yang, H. Yan, Y. Li, P. Wen, and F. Yang, "Secure zonotopic set-membership state estimation for multirate complex networks under encryption-decryption mechanism," *IEEE Trans. Autom. Control*, vol. 69, no. 8, pp. 5109–5124, Aug. 2024.

[43] M. Yao, D. Chen, J. Hu, and N. Yang, "Set-membership state estimation for time-varying complex networks: Two zonotopic design methods," *Int. J. Gener. Syst.*, vol. 54, no. 2, pp. 218–239, 2025.

[44] M. Ye, J. Liu, B. D. O. Anderson, C. Yu, and T. Başar, "Evolution of social power in social networks with dynamic topology," *IEEE Trans. Autom. Control*, vol. 63, no. 11, pp. 3793–3808, Nov. 2018.

[45] J. Yin, F. Yan, Y. Liu, G. He, and Y. Zhuang, "An overview of simultaneous localisation and mapping: Towards multi-sensor fusion," *Int. J. Syst. Sci.*, vol. 55, no. 3, pp. 550–568, 2024.

[46] Y. Zhang, N. Xia, Q.-L. Han, and F. Yang, "Set-membership global estimation of networked systems," *IEEE Trans. Cybern.*, vol. 52, no. 3, pp. 1454–1464, Mar. 2022.

[47] Y. Zhang, C. Ran, and S.-L. Sun, "Robust fusion filter for networked uncertain descriptor systems with colored noise and cyber-attacks," *Signal Process.*, vol. 227, art. no. 109724, 2025.

[48] Y. Zhang, L. Zou, Y. Wang, and Y.-A. Wang, "Estimator design for complex networks with encoding decoding mechanism and buffer-aided strategy: A partial-nodes accessible case," *ISA Trans.*, vol. 127, pp. 68–79, 2022.

[49] Z. Zhang, X. He, and D. Zhou, "Active fault diagnosis for uncertain LPV systems: A zonotopic set-membership approach," *IEEE Trans Automa. Sci. Eng.*, vol. 21, no. 4, pp. 5110–5120, Oct. 2024.

[50] L. Zhao and B. Li, "Adaptive fixed-time control for multiple switched coupled neural networks," *Int. J. Netw. Dyn. Intell.*, vol. 3, no. 3, art. no. 100018, 2024.

[51] Z. Zhao, J. Liang, Y. Wang, and Y. Zhang, "H_∞ filtering for networked systems: A buffer-aided strategy," in *Proc. 2024 39th Youth Acad. Annu. Conf. Chin. Assoc. Automa.*, Dalian, China, Jun. 7–9, 2024, pp. 398–403.

[52] Z. Zhao, Z. Wang, and L. Zou, "Sequential fusion estimation for multirate complex networks with uniform quantization: A zonotopic set-membership approach," *IEEE Trans. Neural Netw. Learn. Syst.*, vol. 35, no. 4, pp. 5764–5777, Apr. 2024.

[53] Z. Zhao, Z. Wang, L. Zou, Y. Chen, and W. Sheng, "Event-triggered set-membership state estimation for complex networks: A zonotopes-based method," *IEEE Trans. Netw. Sci. Eng.*, vol. 9, no. 3, pp. 1175–1186, May 2022.

[54] C. Zheng, H. Fu, J. Bai, X. Meng, and Y. Chen, "FlexRay protocol based distributed nonfragile dissipative filtering of state-saturated switched stochastic systems," *Int. J. Syst. Sci.*, vol. 55, no. 4, pp. 714–727, 2024.

[55] M. Zhu, R. Wang, and X.-M. Sun, "The optimal distributed weighted least-squares estimation in finite steps for networked systems," *IEEE Trans. Circuits Syst. II, Exp. Briefs*, vol. 70, no. 3, pp. 1069–1073, Mar. 2023.

Zhongyi Zhao (Member, IEEE) received the B.Eng. degree in electrical engineering and automation in 2016 and the Ph.D. degree in control theory and control engineering in 2023, both from the Shandong University of Science and Technology, Qingdao, China.

He is currently a Postdoctoral Research Fellow with the School of Mathematics, Southeast University, Nanjing, China. From November 2021 to October 2022, he was a visiting Ph.D. student with the Department of Computer Science, Brunel University London, Uxbridge, U.K. His current research interests include networked systems, multi-sensor information fusion, and set-membership estimation.

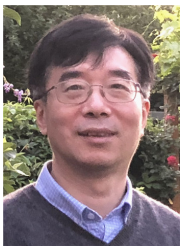

Zidong Wang (SM'03-F'14) received the B.Sc. degree in mathematics in 1986 from Suzhou University, Suzhou, China, and the M.Sc. degree in applied mathematics in 1990 and the Ph.D. degree in electrical engineering in 1994, both from Nanjing University of Science and Technology, Nanjing, China.

He is currently a Professor of Dynamical Systems and Computing in the Department of Computer Science, Brunel University London, U.K. From 1990 to 2002, he held teaching and research appointments in universities in China, Germany and the U.K. Prof. Wang's research interests include dynamical systems, signal processing, bioinformatics, control theory and applications. He has published a number of papers in international journals. He is a holder of the Alexander von Humboldt Research Fellowship of Germany, the JSPS Research Fellowship of Japan, William Mong Visiting Research Fellowship of Hong Kong.

Prof. Wang serves (or has served) as the Editor-in-Chief for *International Journal of Systems Science*, the Editor-in-Chief for *Neurocomputing*, the Editor-in-Chief for *Systems Science & Control Engineering*, and an Associate Editor for 12 international journals including IEEE Transactions on Automatic Control, IEEE Transactions on Control Systems Technology, IEEE Transactions on Neural Networks, IEEE Transactions on Signal Processing, and IEEE Transactions on Systems, Man, and Cybernetics-Part C. He is a Member of the Academia Europaea, a Member of the European Academy of Sciences and Arts, an Academician of the International Academy for Systems and Cybernetic Sciences, a Fellow of the IEEE, a Fellow of the Royal Statistical Society and a member of program committee for many international conferences.

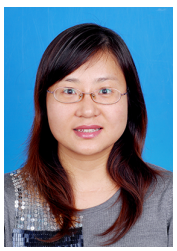

Jinling Liang received the B.Sc. and M.Sc. degrees in mathematics from Northwest University, Xi'an, China, in 1997 and 1999, respectively, and the Ph.D. degree in applied mathematics from Southeast University, Nanjing, China, in 2006.

She is currently a Professor in the School of Mathematics, Southeast University, Nanjing, China. She has published around 90 papers in refereed international journals. Her current research interests include stochastic systems, complex networks, robust filtering and bioinformatics. She serves as an associate editor for several international journals.

Wenying Xu (Senior Member, IEEE) received M.S. degree in Applied Mathematics from Southeast University, Nanjing, China, in 2014, and the Ph.D. degree in applied mathematics from the City University of Hong Kong, Hong Kong, in 2017.

Prof. Xu is currently a Professor in the School of Mathematics, Southeast University, China. Prior to her current position, she was a Post-Doctoral Fellow in Potsdam Institute for Climate Impact Research, Potsdam, Germany from 2019 to 2021, and a Research Fellow in the School of Electrical and Electronic Engineering, Nanyang Technological University, Singapore from 2017 to 2018, respectively. From May 2015 to Aug. 2015 and from Oct. 2019 to Dec. 2019, she severed as an Academic Visitor in the Department of Computer Science, Brunel University London, U.K. Her current research interests include cyber-physical system, game theory in networks, distributed event-triggered control, and distributed cooperative control.

Prof. Xu serves as an Associate Editor for *IEEE Transactions on Systems, Man, and Cybernetics: Systems* and *Systems & Control Letters*; and a Senior Member of *IEEE*. Prof. Xu was a recipient of an Alexander von Humboldt Fellowship in 2018.